Applications of Heteroatom-Based Oligomers and Polymers in Optoelectronics

Matthew P Duffy, Pierre-Antoine Bouit, Muriel Hissler

Applications of Heteroatom-based Oligomers and Polymers in Optoelectronics

*Matthew P. Duffy, Pierre-Antoine Bouit, Muriel Hissler**

Phosphore et Matériaux Moléculaires, UMR 6226, CNRS-Université de Rennes 1, Univ. Rennes, CNRS, ISCR - UMR 6226, F- 35000 Rennes, France

muriel.hissler@univ-rennes1.fr

This book chapter highlights the different kinds of heteroatom based materials that have been used in electronic devices, such as organic light-emitting diodes (OLEDs), organic photovoltaic cells (OPV cells), dye-sensitized solar cells (DSSCs), organic field-effect transistors (OFETs), and electrochromic cells.
Nowadays, new materials with specific properties are still needed for the development of efficient and easily processable organic devices. The control of their properties can be achieved by varying the chemical composition of the conjugated systems and a fruitful approach involves the incorporation of heteroatoms into the backbone of conjugated frameworks.

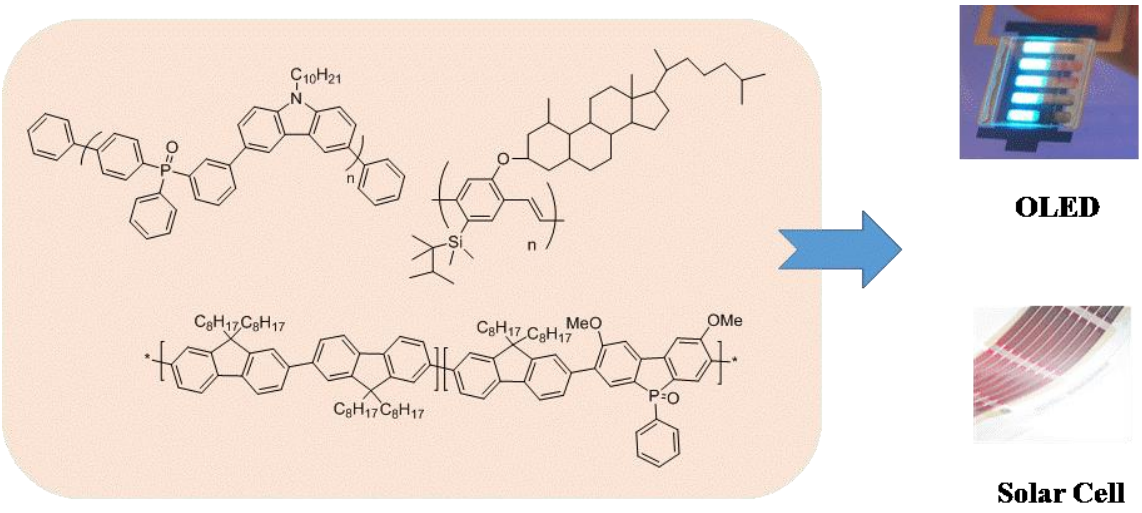

Introduction

Organic semi-conductors (i.e. small molecules, oligomers, and polymers) are by far the most promising functional materials for applications in less expensive and flexible electronic devices such as light emitting diodes (OLED's),

field effect transistors (OFET's) or photovoltaic solar cells.[1] This interest is mainly due to the possibility of tailoring their physical properties and supramolecular organization *via* molecular structural variations.[1] For example, the optical and electronic properties of organic semi-conductors depend on the chemical structure of the conjugated oligomer/polymer carbon backbone (HOMO-LUMO gap, electronic density…) and the interaction between the individual molecules (supramolecular arrangement, morphology). Predictive structure-property relationships can be established and the optimization of physical properties to suit a desired function is possible via chemical engineering at the molecular level. This process is nicely illustrated by the development of advanced electroluminescent organic materials following the seminal reports of efficient organic light emitting diodes (OLEDs) based on small molecules and conjugated polymers.[2] Still today, new materials with specific properties are under investigation for the development of efficient and easily manufacturing organic devices. The control of their properties can be achieved by varying the chemical composition of conjugated systems, and due to the high flexibility of organic synthesis, many strategies can be considered to diversify these structures. A fruitful approach involves the incorporation of heteroatoms into the backbone of conjugated frameworks,[3] with two main approaches being possible for the development of polymers. The first involves the use of heterocyclopentadiene subunits since their electronic properties depend on the nature of the heteroatoms (Figure 1). Metalloles of Group 14 elements (siloles, germoles, stannoles) exhibit a high electron affinity[4], whereas those of Groups 15 (pyrrole) and 16 (furan, thiophene) behave as electron-rich aromatic pi-systems[5] and the phosphole can be regarded as a chameleon like structure combining the two properties.[7]

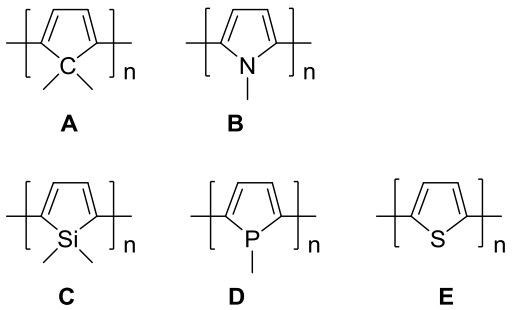

Figure 1. Poly(heterocyclopentadienes).

Based on these metallaloles, a large number of oligomers and polymers have been developed offering a combination of novel electronic properties, excellent stabilities and structural diversity. It can be highlighted that polymers including the heavier elements have much narrower bandgaps than their corresponding second row analogues (Figure 1: silole *versus* cyclopentadiene, phosphole versus pyrrole). This effect is particularly prominent for the group 15 derivatives with the estimated bandgap for poly(phosphole) being half of that of poly(pyrrole). The second strategy is to replace the vinylene bridges of poly(p-phenylene

vinylene), PPV, by a heteroatom possessing a lone pair that can participate in the π-conjugation.[6] Representative examples of this class of derivatives are the polyanilines and poly(p-phenylenesulfides). In résumé, the introduction of heteroatoms and/or heterocycles allows the emergence of new electronic and geometric properties directly related to the nature of the item.[7] Furthermore, the incorporation of heavier heteroatoms-based polymers into devices has been achieved only since 10-15 years, despite decades of research on such species. In this chapter, we will highlight the different kinds of heteroatom based materials that have been used in electronic devices, such as organic light-emitting diodes (OLEDs), organic photovoltaic cells (OPV cells), dye-sensitized solar cells (DSSCs), organic field-effect transistors (OFETs) and electrochromic cells.

Organic light emitting diodes (OLED)

Organic light-emitting diode technology is attracting considerable attention due to their use in flat-panel displays and solid-state lighting.[1,2] An OLED is a flat light-emitting technology based on small molecules or polymers able to generate electrically stimulated emission of light. The multilayer structure of an OLED consists of several organic layers (hole-transport layer (HTL), emissive layer (EML), electron transport layer (ETL)) sandwiched between two electrodes (transparent conducting oxide anode and a metallic low work function cathode), as depicted in Figure 2.[1,8] When a voltage is applied between the electrodes, holes are injected into the HTL layer from the anode and electrons are injected into the ETL layer from the cathode. Then, these charge carriers migrate under the applied electric field, generally by a hopping processes and recombine to form singlet and triplet excitons (bound excited-state electron-hole pairs). The location of the recombination zone in the diode is a function of the charge mobility of the organic material as well as of the electric field distribution. After diffusion, the exciton recombines and a photon is emitted.

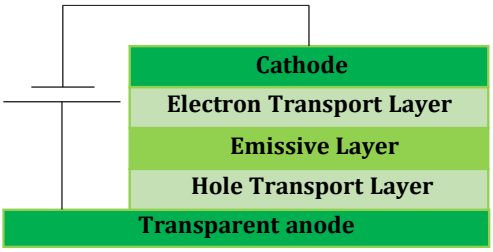

Figure 2. OLED structure.

In order to evaluate the performance characteristics of an OLED, a set of electrical and optical characterizations can made. The electrical parameters can be determined from *I-V-L* (current-voltage-luminance) characteristics.[9]

(1) The internal quantum efficiency η_{int} is the ratio of the total number of photons generated within the device to the number of injected charges;

$$\eta_{int} = \frac{Ninternal\ emitted\ photons}{Ninjected\ charges} = \beta \cdot \rho S/T \cdot \eta PL$$

(2) The external quantum efficiency η_{ext} is the ratio of the total number of photons emitted from the device into the viewing direction to the number of injected charges;

$$\eta_{ext} = \eta_{int} \cdot \eta_{out} = \eta_r \chi \cdot \phi_{PL} \cdot \eta_{out}$$

η_r, probability that holes and electrons recombine to form excitons.
χ, probability to produce emitting species
ϕ_{PL}, fluorescence or phosphorescent quantum yield
$\eta_{out,}$ fraction of generated photons emitted by the device

(3) the luminous efficiency η_L in candelas per ampere (cd/A) is the ratio of the luminous intensity in the forward direction and the current through the device

$$\eta_L = \frac{S \cdot L}{I}$$

L, Luminance in $Cd.m^{-2}$
S, Surface of the diode in m^2
I, Current in A.

(4) The luminous power efficiency or luminous efficacy η_P in lumen per watt (lm/W) represents the output light power from a device per electrical power input (measured in watts). The efficacy of a light source takes into account the sensitivity of human vision to the different wavelengths of the visible spectrum.

$$\eta_P = \frac{\eta_L \cdot \pi \cdot}{V}$$

V, Working voltage

Since high–quality light is important for illumination, it is important to qualitatively define the color quality of OLEDs. Three different light output characteristics can be used:

(i) the Commission Internationale d'Eclairage (CIE) chromaticity coordinates (x,y) (chromaticity), locate the emission color in a chromaticity diagram allowing an optical comparison of all different sources. The CIE chromaticity coordinates of pure white light are (0.33,0.33)

(ii) the Correlated Color Temperature (CCT) is the color appearance of a light source, measured by the source's chromaticity in reference to the blackbody locus

(iii) the Color Rendering Index (CRI) is a number ranging from 0 to 100 measuring how accurate the colors of objects can be rendered under a given illumination condition

As already mentioned, the multilayer structure of an OLED consists of several organic layers (hole-transport layer (HTL), emissive layer (EML), electron transport layer (ETL)) playing a specific role in the production of light via electroluminescence (EL). Thus, each organic material must fulfill certain requirements. Overtime, scientists have begun to understand how the manipulation of the chemical structure of these heteroatomic oligomers/polymers allows the flexibility of fine-tuning the chemical, optical, and electrochemical properties of these systems, and have begun incorporating them into OLED structures.

Application as Charge-Transport Layer

A charge-transport layer must facilitate the charge transport and injection from the device's electrodes to the active layer of the OLED. [8,9] In order to fulfill these requirements, different heteroatom-based materials have been synthesized and studied. For example, phosphine oxide-based materials present interesting electron-transport and injection capabilities, hole and exciton blocking properties, as well as good morphological stability. At the beginning arylphosphine **1** (Figure 3)[10] was the first phosphine oxide-based material to be used as a hole-transporting layer (HTL) and exhibited better performances than its nitrogen counterpart in an OLED. Later, it was discovered that π-extended phosphine oxides (Figure 3)) possessed good electron–transporting abilities due to the highly polar PO group.[11]

For example, triphenylphosphine oxide was used to replace tris-(8-hydroxyquinoline)aluminium (Alq_3) allowing to reduce the driving voltage for luminance output. Then, chemical engineering was performed around the phosphine oxide unit leading to more efficient ETL. For example, the phosphine oxide unit was attached to pyrene (**2**, Figure 3)[12] or spirobifluorene (**3**-**6**, Figure 3) π-systems.[13] The nature of the substituents plays an important role for improving the OLED performance. The pyrene substituents allows an enhancement of the conductivity due to it's packing ability and the spirobifluorene in SPPO2 **5** and SPPO21 **6** (Figure 3) facilitates the electron injection, allowing direct injection from the Al cathode.[14] SPPO21 **6** has also shown to be an effective ETL in an OPV cell (ITO/PEDOT:PSS/P3HT:PCBM/SPPO21 **6**/Al).[15] The compound **6** protects the active polymer from Al diffusion into the active layer leading to higher performances, and a lowering of the open circuit voltage (V_{oc}) is observed since the coordination ability of the phosphine oxide onto the Al surface leads to band

bending. It was a more effective interlayer than LiF in terms of open-circuit voltage and efficiency.

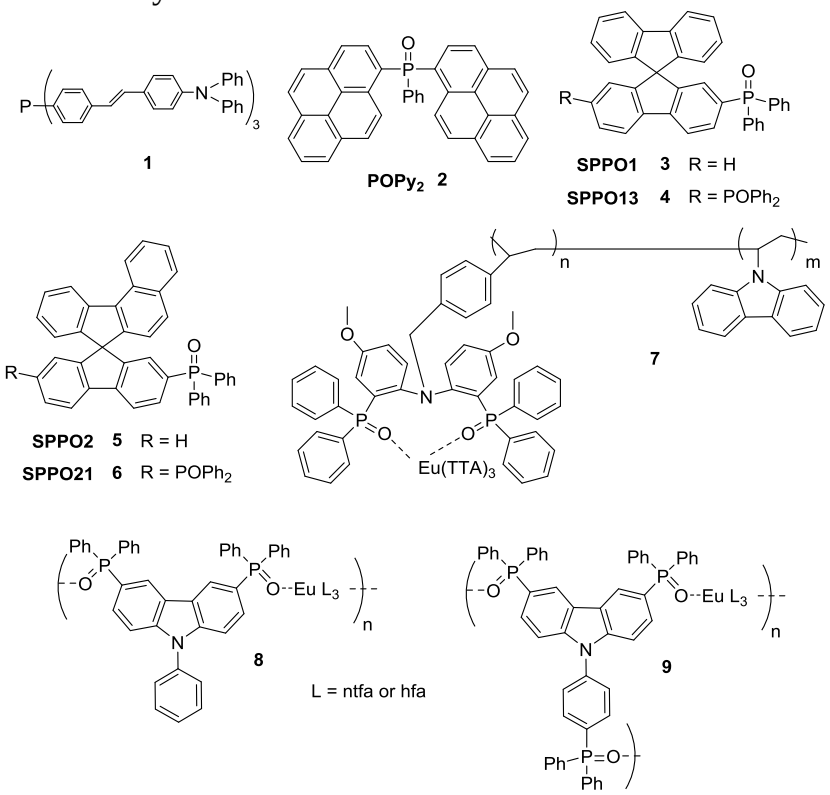

Figure 3. Phosphine materials as charge-transport and injection layers.

Since phosphine oxide units have low vibrational frequency leading to the suppression of nonradiative transitions via vibrational relaxation, this unit is used as a ligand for the formation of lanthanide polymers having high quantum yields. For example, Europium complexes-based polymers **7**, **8** and **9** including bidentate and tridentate phosphine oxides with carbazole units, respectively, have been prepared and studied. The carbazole unit plays the role of hole transporter in the emitting layer and the electron-injection ability of phosphine oxide compounds is preserved leading to an effective EL device reaching luminance of 149 and 188 cd. m^{-2} with compounds 7 and 8, respectively.[16]

Another efficient class of organophosphorus electron transporters are π-conjugated phospholes. Tsuji/Sato/Nakamura et al. synthesized benzo[b]phosphole oxides **10a** and sulfides **10b**, Figure 4 and tested them as electron transporting layers in OLEDs.[17] They showed that 11b had a higher electron mobility than **10a** (**10a**: 5×10^{-6} V^{-1} s^{-1}, **10b**: 2×10^{-3} V^{-1} s^{-1}) indicating that the decrease in polarity from P=O to P=S improved the electron mobility by preventing electron trapping with the highly polarized P=O sections. They co-deposited **10a** or **10b** with cesium (Cs) to form an electron-transport material (ETM), using the device configuration [ITO/ PEDOT:PSS/ α-NPD/ Alq_3/ ETM:Cs /Al]. The device using **10b** as the ETM had the best performance with a luminance of 1000 cd m^{-2}, driving voltage of 5.0 V, luminance efficiency of 1.8 lm W^{-1}, and a current efficiency of 2.8 cd A^{-1}.

Compounds **10a,b**, **11a,b** and α,α'-diarylacenaphtho[1,2-*c*]phospholes **12a-d** (Figure 4) have been used as ETL in organic photovoltaic devices.[18] The benzophosphole sulfides **10b** and **11b** presenting high glass-transition temperatures and resistance towards crystallization, have performed the best in OPV device featuring a porphyrin donor and fullerene acceptor with a device configuration: [ITO/PEDOT:PSS/BP/BP:SIMEF/SIMEF/ETL/Al]. (V_{OC} = 0.71 V, J_{SC} = 10.8 mA cm^{-2}, FF = 0.61, and a η = 4.6%, with **11b**: V_{OC} = 0.72 V, J_{SC} = 10.4 mA cm^{-2}, FF = 0.61, and a η = 4.6%) (see photovoltaic section for definitions of parameters).

The molecular engineering performed around the acenaphtho[1,2-*c*]phospholes by tuning the α-aryl substituent modified the degree of π-conjugation, electron-accepting ability, solid-state packing, and thermal stability of the phosphole materials. The best performing device [ITO/PEDOT:PSS/ P3HT:$IC_{70}BA$/ETL/Al] contained **12b** as the ETL (V_{OC} = 0.76 V, J_{SC} = 8.8 mA cm^{-2}, FF = 0.62, and a η = 4.2%). These examples emphasize the potential of π-conjugated phosphole oxides and sulfides as charge-transport materials for organic electronics.

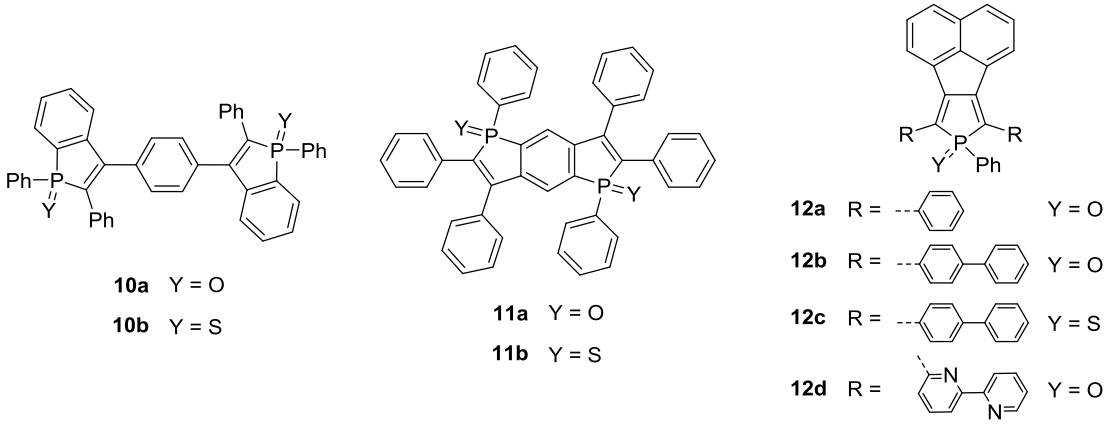

Figure 4. ETL Phosphole-based molecules used as charge transport layers.

Besides phosphole rings, silole rings can also be used for the development of electron transport materials.[19] The silole ring presents a high electron affinity and a low LUMO energy since this ring presents a σ*-π* conjugation between the σ* orbitals of the exocyclic bonds on silicon and the π*orbitals of the butadiene moiety (negative hyperconjugation). Compounds **13**-**15** (Figure 5) present a higher electron affinity compared to Alq_3 leading to higher electron mobility and improved EL efficiencies. [20] For example, compound **14** presents an electron mobility higher than Alq_3 (2. 10^{-4} cm^2/(Vs)) and OLEDs including compound **14** as the ETM present half-life time of the luminance nearly 3 times longer than for a device without it. It is likely that the use of compound **14** as an ETM improves the charging and thus the longevity.

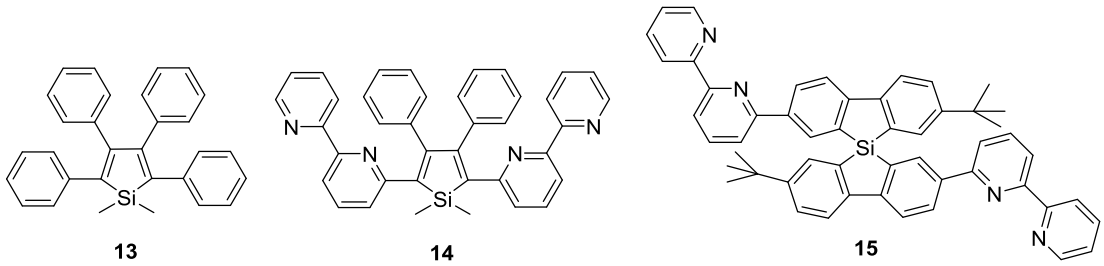

Figure 5. Silole-based ETLs used as charge transport layers.

Different boron-based ETMs have been developed. For example, tris-[3-(3-pyridyl)mesityl]borane **16** and 5,5”-bis-(dimesitylboryl)-2,2’:5’,2”-terthiophene **17** (Figure 6) have been used as ETMs in OLEDs. Compared with OLEDs built with a conventional ETM (Alq_3), higher luminance and larger current density were achieved with the two compounds as the ETM.[21]

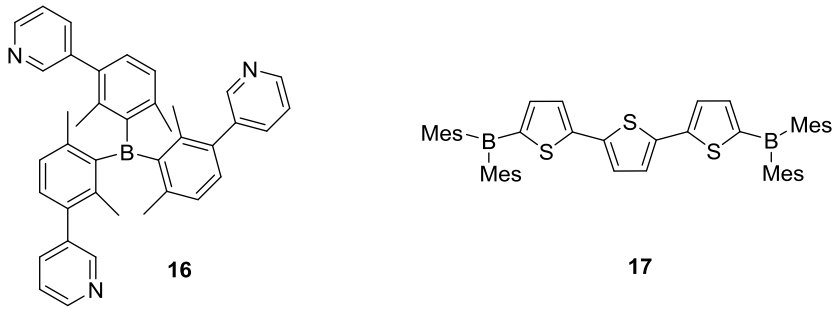

Figure 6. Boron-based ETMs.

Application as Host for Phosphorescent Complexes

To be an efficient host material for a triplet emitter in an OLED, the substance must satisfy several requirements: (i) to be both physically and chemically stable, (ii) to be efficient in both, hole- and electron-transporting, (iii) it must contain an appropriate triplet energy level in order to transfer energy to the triplet emitter. The first report of a phosphine oxide based material used as a host for a triplet emitter was in 2006,[22] since then a plethora of PO materials connected to different cores have been studied. Typically, these hosts contain electron-withdrawing and electron-donating groups. The phosphine oxide is electron-withdrawing and facilitates the electron transport. Usually for the electron-donating groups, a tertiary amine is used, as it aides in the hole-transport. Some of the most efficient PO hosts are connected to carbazole groups, which are well known to have good hole-transporting abilities. When compound **18** (Figure 7) was used as the host for a sky blue PhOLED (dopant FIrpic) it achieved a high external quantum efficiency of 23.9 %, with a low driving voltage.[23] In the same article, Lee et al. also showed that the position of the phosphine oxides on the carbazole also has a significant effect on the performance of the host. When the phosphine oxides were placed in the 2,7 positions, i.e. **18**, the quantum efficiency increased by more than 50 %, and the power efficiency was significantly

improved, compared to the carbazole with phosphine oxide substituents in the 3,6 positions.

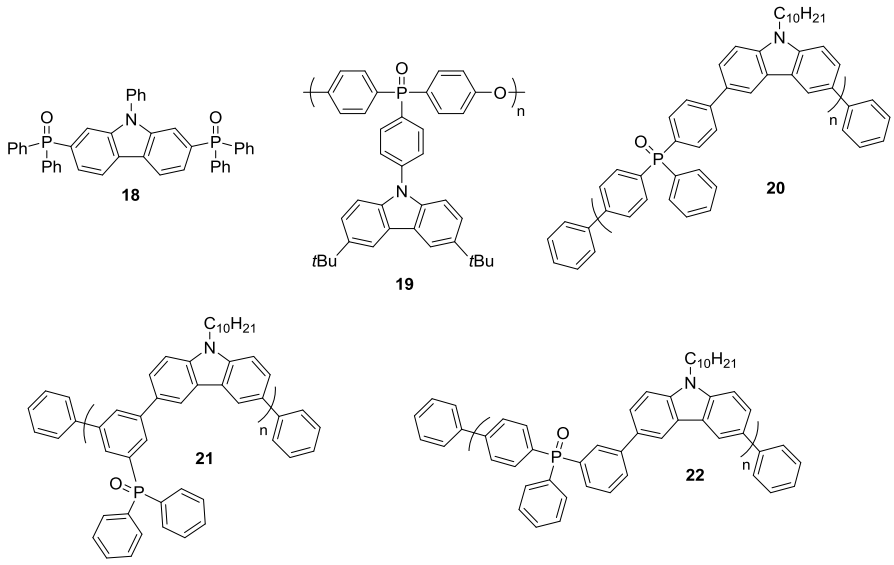

Figure 7. Selected hosts based on phosphine oxides and carbazole.

Different bipolar polymeric hosts **19-22** (Figure 7) based on phosphine oxide and carbazole scaffolds have been synthesized and studied. For example, Ding, Wang et al. showed that the polymer **19** presents a high thermal stability, a high E_T of 2.96 eV and an efficiency of 10.8 % can be reached in an OLED device using FIrpic as the emitter.[24] H.–J. Jiang et al. showed that triphenyl phosphine oxide and carbazole–based polymers **20-22** can be used as host materials for green phosphorescent dopants of PhOLEDs.[25] They fabricated PhOLEDs with the configuration ITO/PEDOT:PSS (40 nm)/host (**20-22**): 5% $Ir(mppy)_3$ (40 nm)/1,3,5-tris(1-phenyl- 1H-benzimidazol-2-yl)benzene (35 nm)/LiF (0.8 nm)/Al (100 nm). The PhOLED including polymer **20** as the host material shows electroluminescent performance with maximum current efficiency of 2.16 $cd \cdot A^{-1}$, maximum external quantum efficiency of 0.7%, maximum brightness of 1475 $cd \cdot m^{-2}$ and reduced efficiency roll-off of 7.14% at 600 $cd \cdot m^{-2}$. The best performance has been obtained with polymer **20**. This data indicates that the introduction of triphenyl phosphine oxide into the polycarbazole main chain through different linking models has been an effective way to adjust the thermal stability, photoelectric properties and device performance of polymer host materials.

Phosphazenes are compounds where P and N are linked by an alternation of single and double bonds. However, this compound should be considered as a ylide structure ($-P^+-N^-$) and not as a π-conjugated framework (see chapter "Synthesis of polymers containing group 15 elements") .[26] This backbone is easily functionalized to afford linear polyphosphazenes or cyclic phosphazenes. These polyphosphazenes and cyclic phosphazenes are interesting candidate as hosts for triplet emitters since they possess a relatively high HOMO-LUMO gap. Simple aryl-substituted cyclic phosphazenes such as **23** (Figure 8) were tested

as a matrix for Ir(dbfmi) emitters. Low efficiencies were obtained with these hosts despite balanced charge transport (power efficiency max = 7.6 lm W^{-1}).[27] Carbazole-functionalized derivatives (for example **24**, Figure 8) were then designed.[28] The triplet level of this amorphous matrix was evaluated at 3 eV, which is compatible with FIrpic and $Ir(mppy)_3$. Multilayered OLEDs [ITO/PEDOT:PSS/poly-TPD/EML/BCP/BCP:Cs_2CO_3/Al] with FIrpic as the emitter showed twice the luminance/PCE of a PVK reference device that was prepared with this host. These two examples show that chemical diversity can be easily introduced on the phosphazene core to obtain hosts for PhOLEDs. It is particularly interesting to note that in both cases the matrices are amorphous and thermally stable.

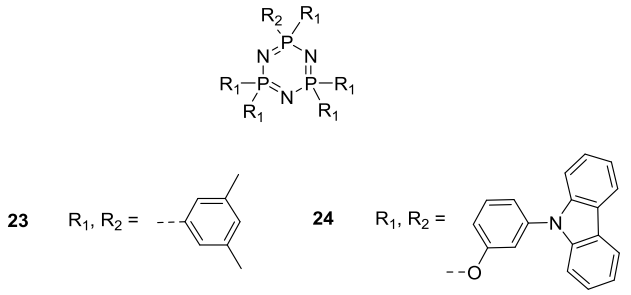

Figure 8. Phosphazene derivatives used in OLEDs.

Application as Emitting Materials

A large number of heteroatom based-oligomers and polymers presenting very interesting emissive or charge-transport properties,[29] has been synthesized but only few of them have been incorporated in devices. Most of the emitters used in OLEDs contains mainly phosphorus and silicon.

Phosphine oxide-based materials are interesting emitters because they are thermally stable and have good morphological stability. Furthermore, they incorporate a pyramidal phosphorus which prevents π-stacking in the solid state and therefore promotes solid-state emission. A highly efficient light-blue emitter **25** (Figure 9) was synthesized and used to construct a double-layer device utilizing **25** as the emitting, electron-transporting, and electron-injecting material. An η_{ext} of 4.3% was achieved with chromaticity CIE coordinates (0.15, 0.07).[30]. Ma/Yang et al. synthesized a series of solution-processable linear oligomer emitters consisting of a phosphine oxide center connected to oligo-phenylene/fluorene cores and end-capped with N-phenylnaphthalen-1-amine groups.[31] They constructed solution-processed OLEDs utilizing **26** (Figure 9) as the emitter. A maximum current efficiency of 2.36 cd A^{-1}, a maximum power efficiency of 1.86 lm W^{-1}, and a maximum external quantum efficiency of 2.06 % with CIE coordinates (0.15, 0.11) was achieved for the deep blue OLED. Later Yang/Wu et al. developed two-dimensional oligofluorenes connected to a central triphenyl phosphine oxide **27-29** (Figure 9).[32] The device utilizing **29** as the emitter had the best performance, with a maximum current efficiency of 1.88 cd

A^{-1}, and η_{ext} of 3.39% with CIE coordinates (0.16, 0.09). This example highlights the increase in efficiency based on 2D frameworks over their 1D counterparts. Ding/Wang et al. generated highly efficient blue electrophosphorescent polymers composed of a fluorinated poly(arylene ether phosphine oxide) backbone with grafted carbazole and FIrpic units.[33] The best performing device utilized **30** (Figure 9) as the emitter and achieved a luminous efficiency of 19.4 cd A^{-1}, an η_{ext} of 9.0 %, and CIE coordinates (0.18, 0.33). Although the majority of the phosphorescence comes from the FIrpic moieties, the poly(arylene ether phosphine oxide) backbone plays a definite role in the charge transport of the emissive polymer. In a further study, the authors introduced an additional yellow phosphorescent emitter [$(fbi)_2Ir(acac)$] into the polymer backbone and achieved a white OLED (WOLED).[34] The simultaneous blue and yellow triplet emission allowed the generation of white electroluminescence, and the device had a luminous efficiency of 18.4 cd A^{-1}, an η_{ext} of 7.1%, and CIE coordinates (0.31, 0.43).

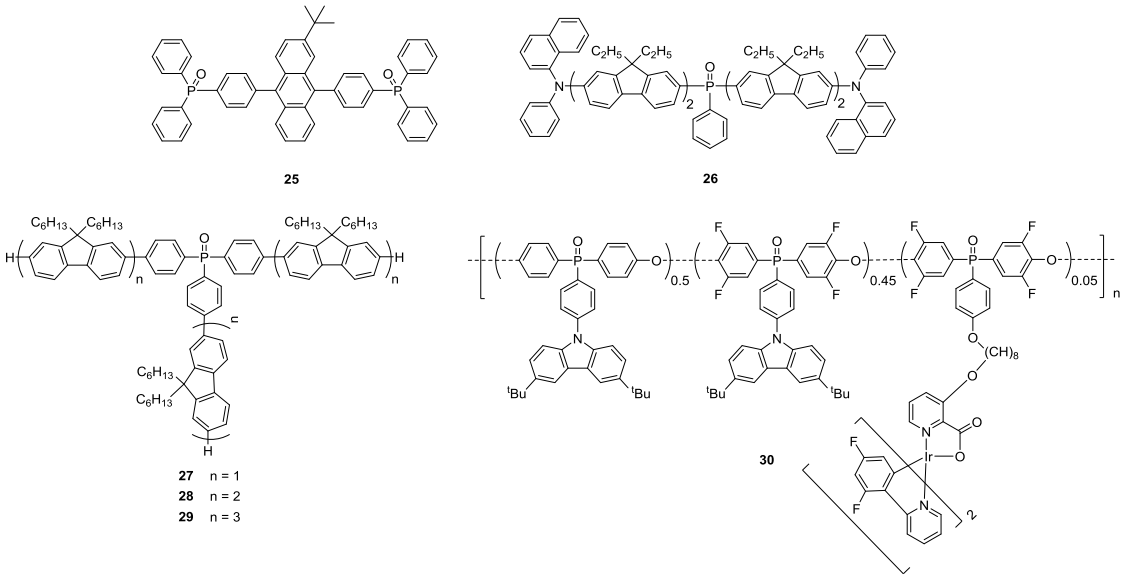

Figure 9. Examples of phosphine oxide-based emitters.

Several phosphole based polymers have been synthesized and studied.[29f-h] They are efficient emitters and/or charge transporters but only few of them have been used as emitters in OLEDs. Phosphole-based oligomers have been used for the first time, as emissive layer in OLEDs in 2003 by Réau/Hissler et al..[35] For example, they demonstrated that the compound **31** (Figure 10) can be used as an OLED emitter.[36] The devices employed in this study had the following configuration: [ITO/PEDOT:PSS/α-NPD/ emissive layer : **31** /Alq_3/Mg:Ag/Ag] using Alq_3 as an ETL and α-NPD as a HTL. The different organic layers were deposited by thermal evaporation under high vacuum. The thermal stability of the thioxo derivative **31** (Figure 9) allowed to get homogeneous thin films having an emission wavelength centered at 550 nm and good device performance (MB = 38,000 cd m^{-2}, η_{max}= 0.80). Since the phosphole derivative **31** presents interesting hole-transport properties and an emission that overlaps with the absorption spectrum of the highly red fluorescent dye 4-(dicyanomethylene)-2-

tert-butyl-6-(1,1,7,7-tetramethyl-julolidin-4-yl-vinyl)-4H-pyran (DCJTB), it was used as host for a red emitter.[35,36] Although the dopant concentration (1.4 % wt) was not optimized, this approach led to an important enhancement of the η_{ext} (1.83%) and a maximum brightness of 37,000 cd m^{-2} (λ_{max} = 617 nm).

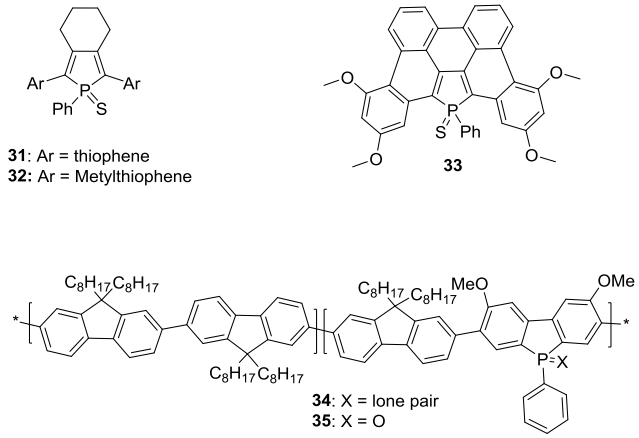

Figure 10. Phosphole derivatives as emitters in OLEDs and WOLEDs.

Phosphole emitters also appeared as original materials for the construction of WOLEDs. Since the organophosphorus compounds are redox and thermally stable, and present an orange emission, Réau/Hissler et al. co-evaporate **32** (Figure 10) with a blue emitter, 4,4'-bis(2,2'-diphenylvinyl)biphenyl (DPVBi) for the construction of the active layer in WOLEDs. Effectively, white emission could potentially be obtained by combining orange and blue emissions, if the ratio of the two colors is correct.[37] It is important to note that, the absorption spectra of phosphole-thiophene derivatives span the 320-524 nm range, and overlap with the emission spectrum of DPVBi to a large extent, potentially allowing energy transfer from the DPVBi host to the phosphole dopants. First, Réau/Hissler et al. developed a multilayer WOLED on a glass substrate with a configuration of [ITO/CuPc (10 nm)/α-NPB (50 nm)/emissive layer :doped-DPVBi (50 nm)/Alq_3 (10 nm)/LiF (1.2 nm)/Al (100 nm)].[38] Doping of the blue matrix with 0.2% of compound **32** leads to an OLED exhibiting a small turn-on voltage (5.2V) with current and power efficiencies of 7.0 cd A^{-1} and 2.3 lm W^{-1}, respectively. Its electroluminescent spectrum presents well-balanced emission characteristics of the DPVBi (452 nm, FWHM = 70 nm) and of the dopant **32** (548 nm, FWHM = 115 nm). The resulting CIE coordinates (0.31,0.39) are close to those of pure white light (0.33,0.33) and are independent of the driving current.

Fully planarized phosphorus-containing polycyclic aromatic hydrocarbon[39] (**33** Figure 10) presents high luminescence in the orange-red region in dilute solutions and this fluorescence remains high in a solid matrix. This compound has been used as orange dopant in a blue emitting matrix for the development of WOLEDs.[39] The WOLEDs having the configuration [ITO/ CuPc/α-NPD/EML/DPVBi/BCP/Alq_3/LiF/Al] exhibit a white emission as evidenced by the CIE coordinates when the EML is generated by co-subliming **33** (0.8 wt%) with the α-NPD. The device utilizing emitter **33** in the emissive layer (EL = α-

NPD: **33** (1.1 wt%)) had a turn-on voltage of 5.55V, brightness of 1122 cd m^{-2}, η_{ext} of 1.67%, power efficiency of 0.96 lm W^{-1}, current efficiency of 3.69 cd A^{-1}, and the CIE coordinates (0.32, 0.37).

The first investigation of the potential application of low molecular weight dibenzophospholes in OLEDs by vacuum sublimation was unsuccessful, as the device characteristics showed instability with increasing driving current.[38] In 2008, Huang et al. reported the synthesis of phosphafluorene (that is, dibenzophosphole) copolymers (**34** and **35**, Figure 10).[40] Since, both polymers were emissive and had high decomposition temperatures (400°C), they were employed in a polymeric light-emitting diode (PLED) device [configuration: ITO/PEDOT:PSS/polymer/Ba/Al]. The device with **34** as the EML, presented blue EL (CIE coordinates: (0.21, 0.24)) with brightness up to 1423 cd.m^{-2} whereas **35** exhibited white emission (CIE coordinates: (0.34, 0.36)), but with lower brightness (142 cd.m^{-2}). The nature of the substituents on the P-atom of the phosphafluorene derivative has a strong impact on the properties of the polymer, changing the blue EL to a white one. All the described examples of a phosphole-based emitters clearly highlight the potential of these materials for the development of OLEDs and WOLEDs.

The cyclic phosphazenes core is an interesting platform which can be easily functionalized by substituents having specific optical properties. For example, pyrene (pyrenic emitters **36** and **37**, Figure 11) and phosphorescent complexes (Ir-complex **38**, Figure 11) have been used to functionalize the cyclic phosphazene core.[41] They all form amorphous thin films with a blue-green emission. Single-layer OLEDs displayed low performances due to the lack of electron-transporting ability of the layers. The use of an ETL (TPBi), improved the properties with the configuration [ITO/PEDOT:PSS/**36-38**/TPBI/Ba:Ag]. The best performing compound was **36** (11,000 cd m^{-2} at 12 V, η_{ext} of 0.72% at 8 V). Phosphorescent **38** has also been incorporated in a PVK matrix, to afford a device [ITO/PEDOT/PSS/PVK:PBD:**38**/TPBI/Ba/Si], with an η_{ext} of 7%. A series of phosphazene-containing dendrimers decorated in the periphery by polyaromatic moieties (e.g., anthracene, pyrene) have been synthesized by Caminade/Majoral et al.[42] Films prepared from the pyrene-decorated dendrimers showed a characteristic excimeric emission. The 4th-generation dendrimer **39** (Figure 11) diluted in a PVK matrix was explored in OLED devices. However, the luminance appeared to be low and the threshold voltage very high (> 20 V).

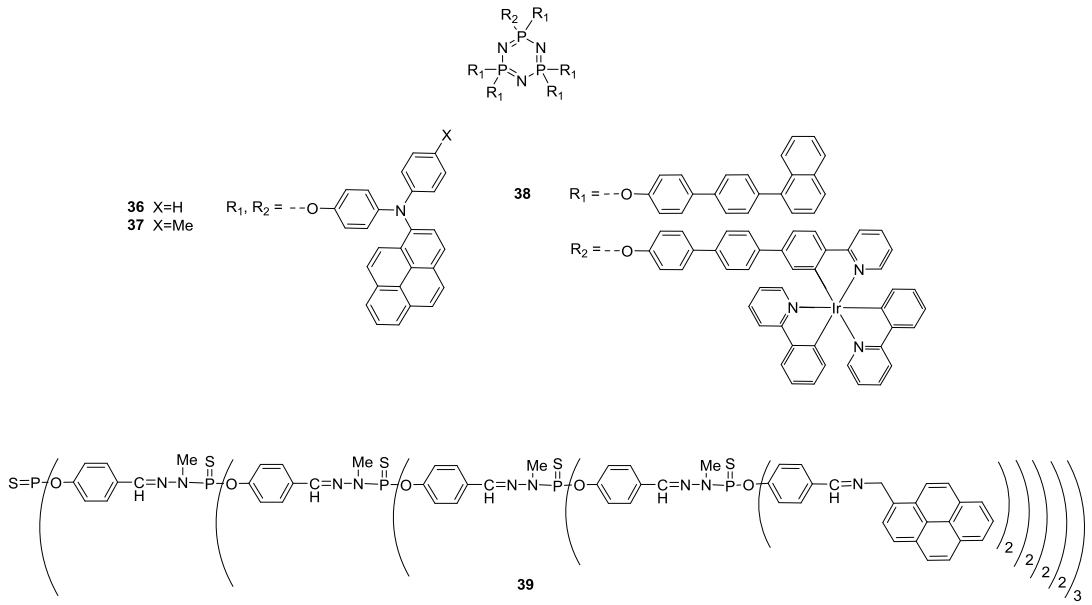

Figure 11. Phosphazene derivatives used as emitter in OLEDs.

Another interesting class of compounds concerns the functionalization of π-systems with silicon atoms, allowing a control of the bandgap and the emission color of the polymers.

Several silyl substituted poly(p-phenylene vinylenes) have been developed and possess high photoluminescence quantum yields. For example Kim et al.[43] synthesized Si-containing polymers **40** (Figure 12) having an emission centered at 515 nm and 550 nm with a photoluminescence quantum yield of 60%. In a single layer OLED (ITO/**40**/Al), the EL emission spectrum is similar to that recorded in solution and η_{ext} reaches 0.05%. The η_{ext} can be improved to 0.2% by using a hole –blocking and electron injecting layer of 2-(4-biphenylyl)-5-(4-tert-butyl-phenyl)-1,3,4-oxadiazole (PBD) between the light emitting layer and the cathode. The introduction of a bulky trialkylsilyl group on PPV (polymer **41**, Figure 12) increases the torsion angle between the phenylene and the vinylene systems leading to a blue shift of the emission.[44] In the device, polymer **41** exhibits light green EL emission with an η_{ext} of 0.3%.[45] Further chemical modifications have been made on the PPV core in order to establish structure-properties relationship. For example, silyl-disubstitued PPVs η_{ext} having different side-chain lengths ranging from C1 to C18 have been synthesized and studied. The silyl-disubstituted PPV **42** having long chains presents better processability and film forming properties. In a single layer OLED (ITO/**42**/Al), η_{ext} reaches only a value of 0.05%. [46] The introduction of more sterically demanding groups like cyclohexyl or phenyl lead also to higher glass temperature and processability but PLEDs with these polymers such as ITO/PVK/**42**/Al emits green-yellow light with a low η_{ext} = 0.08%.[47] PPV derivatives **43-45** (Figure 12) possessing pendant phenyl group substituted with trialkylsilyl substituents in different positions have also been synthesized and studied. The polymer including trialkylsilyl substituent in meta-position of the pendant phenyl **43**[48] has been used as an emitter in the OLED with a configuration: ITO/PEDOT/**43**/Al:Li. Moderate performance (η_{ext} = 0.08%,

maximum of brightness = 570 cd/m^2 at 43 V) have been recorded due to a high –energy barrier between the HOMO band of **43** and the ITO/PEDOT work function. The introduction of trialkylsilyl substituents in the ortho position of pendant phenyl rings don't allow to clearly establish structure/properties relationships since polymers **44** and **45** present a maximum of luminance of 3098 and 383 cd/m^2, respectively, with similar OLED configuration.[49]

The synthesis of PPV including a heavier atom like germanium has been undertaken. A germylated-PPV **46** (Figure 12) has been synthesized by thermoconversion route since classical reactions like the Gilch polymerization usually used for the formation of PPVs gives only insoluble material. The device having the following configuration: ITO/**46**/LiF/Al emits a green light with a moderate efficiency of 0.015 lm/W and a maximum brightness of 600 cd/m^2.[50]

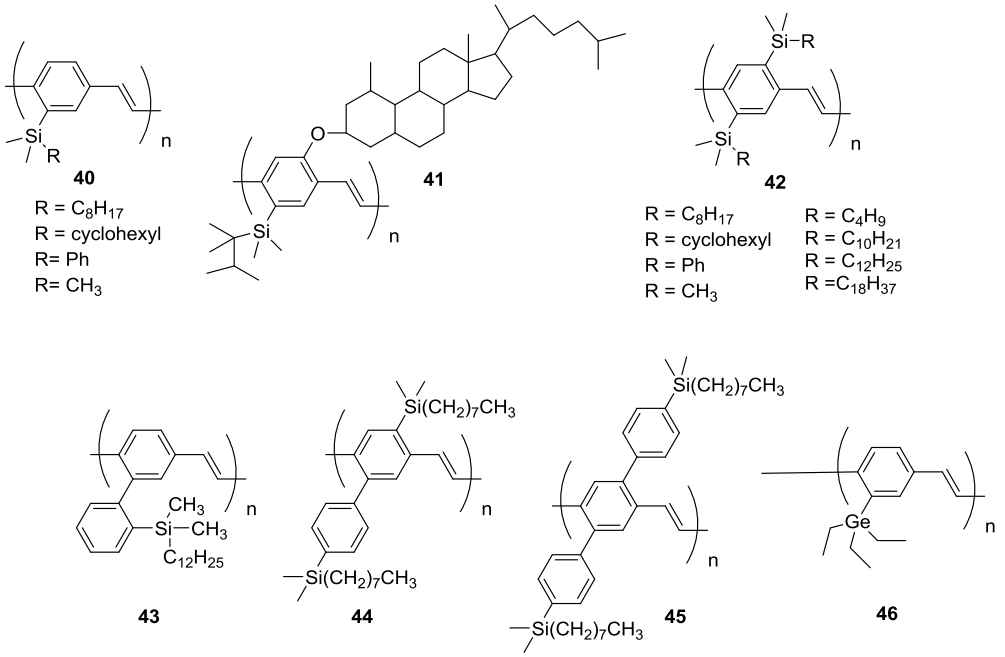

Figure 12. Silyl and germyl-substituted PPVs.

A better control of the HOMO-LUMO gap and the EL properties of PPVs can be achieved with the formation of copolymers. The synthesis of MEH-PPV random polymers with trialkylsilylphenyl **47** (Figure 13) has been achieved by Jin et al.[48] The HOMO and LUMO energy level and the emission color was tuned by adjusting the co-monomer ratio. It was demonstrated that the performance namely the turn on voltage of the OLED is directly related on the gap between the HOMO level of the polymer and the work function of the ITO electrode. The OLED (ITO/**47**/Al:Li) incorporating polymer **47** as the emitter, presents a turn on voltage of 2.3 V, a maximum of brightness of > 19000 cd m^{-2}, η_L of 2.9 lm/W , performance which are higher than the OLED performance built with homo-polymers.

Another way to tune the HOMO level of these polymers is to introduce electron donor substituents. Holmes/Friend et al. synthesized PPV copolymers containing alkoxy- and trialkylsilyl-substituted phenylene rings[51] in a random distribution **48**-**51** (Figure 13). The best performance was observed for devices made with **50**. EL efficiencies were up to 0.72 cd/A with a maximum luminance

of 1384 cd/m^2 at 12 V and turn-on voltages of 4.0 V. In polymer **49**, the presence of oligo(ethylene oxide) pendant groups allowed to create light-emitting electrochemical cells (LECs : ITO/**49**/LiOTf/Al) with an efficiency of 0.5 lm/W.

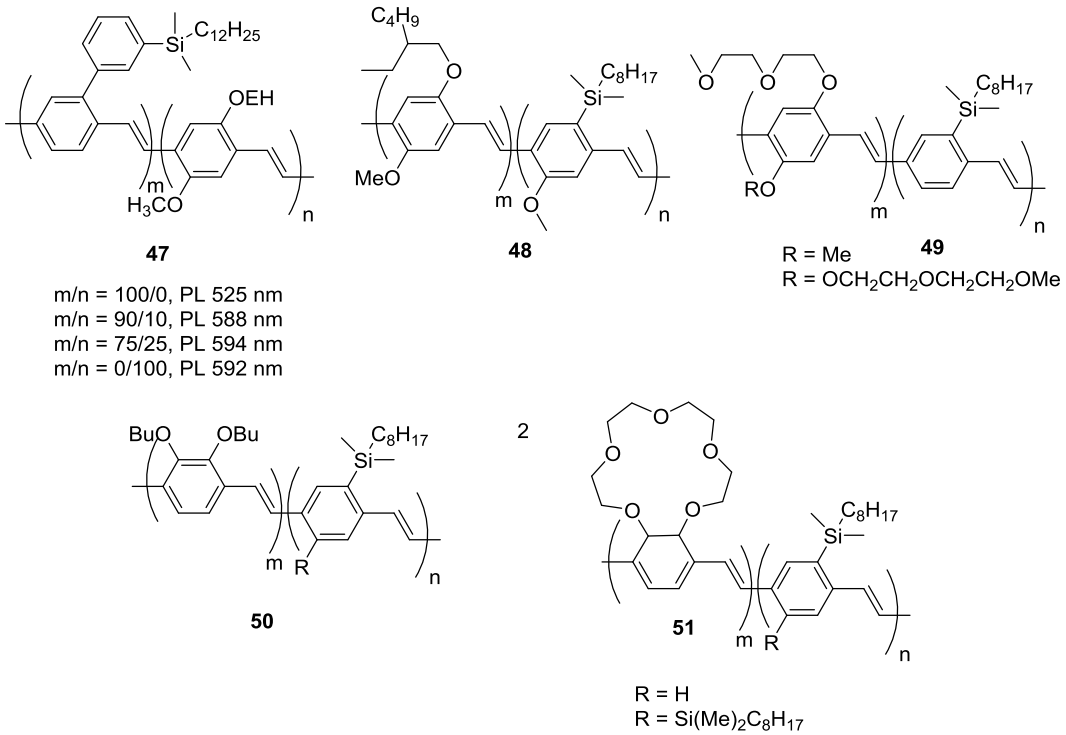

Figure 13. Chemical structures of PPV co-polymers alkoxy- and trialkylsilyl-substituted phenylenes.

There are several ways to control the bandgap of a polymer. One way, consists of the introduction of bulky substituents in order to distort the polymer conjugated backbone (vide supra), another way consists of a precise control of the conjugation lengths. For example, Kim et al. introduced silicon atom in PPV block polymers to confine the conjugation length allowing to obtain blue EL materials **52-55** (Figure 14).[52] Depending on the structure of the polymer **52-55**, emission can be tuned between 410 and 520 nm. Single layer OLED (ITO/polymer/Al) have been constructed with polymers **52** and **54**, and had a turn on voltage of around 7 V. The same approach has been used with polythiophenes. Hadziioannou et al. controlled the conjugation length of oligothiophene blocks by using silanylene units (polymers **56a-d** and **57a-f**, Figure 14) as conjugation interrupters allowing a tuning of the emission from blue to orange. [53] Later, Yoshino et al. were able to change the EL color from green to red by increasing the oligothiophene block length (polymer **56d-h**).[54]

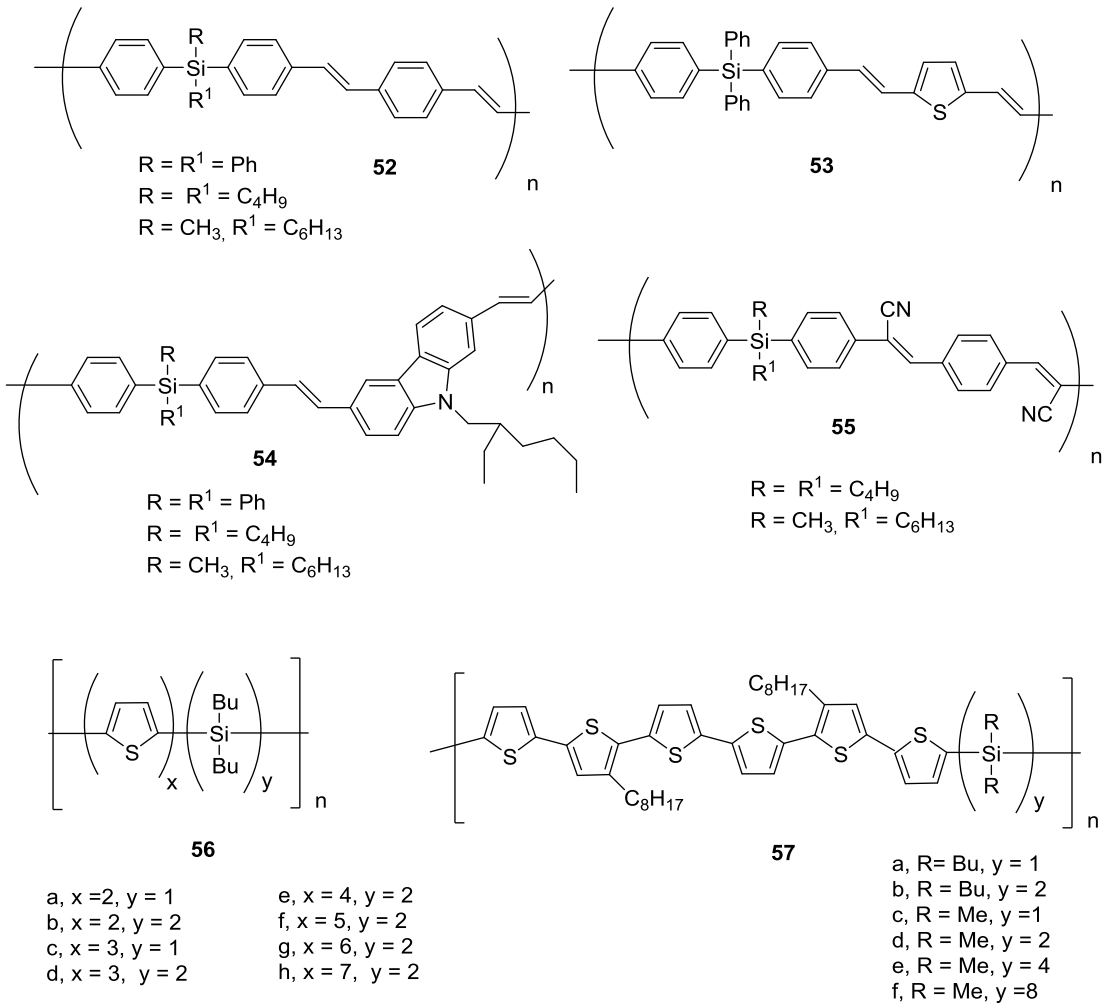

Figure 14. Chemical structures of PPV and polythiophene including silicon atoms.

Besides phosphole rings, silole rings can also be used as building block for the development of emissive materials. Polyphenylsiloles are weakly emissive in diluted solutions but show intense luminescence in the aggregated state. This exalted emission results from stiffening of their molecular structure due to restriction of the intramolecular rotations (RIR) of the peripheral rotors that promotes the radiative decay of the excited state.[55] This observation prompted Chen et al. to develop silole substituted polyacetylenes (PA) **58-60** (Figure 15).[56] As expected, the fluorescence of these polymers **58-60** are very low (ϕ_{PL} < 0.5%) in solution but the PLQY is increased 20 to 50 times in solid state for polymers **59** and **60**. In the case of polymer **58**, an energy transfer is observed from the silole to the PA generating a red-emission (λ_{El} = 664 nm). The introduction of a longer link between the silole unit and the polymer allow to observe the specific emission of the silole at 512 nm. The development of single-layer devices with these polymers gives only moderate EL efficiency (0.013%) due to limited charge-transport processes. The performance can be increased with the development of multi-layer OLEDs (ITO/60-PVK/BCP/Alq_3/Al). A current efficiency of 1.45 cd/A, a η_{ext} of 0.55% and maximum of brightness of 1118 cd/m^2 can be recorded.

Siloles can also be included in the polymeric backbone **58-64** (Figure 15).[57] For example, Liu et al.[57a] used two random silole containing copolymers as emitting layer in a double-layer device (ITO/BTPD-PFCB/**61a,b**/Ca). In the case of polymer **61a**, a maximum brightness of 25,900cd/m^2 and a η_{ext} of 1.64% are recorded. When the 4,4-diphenyldithienosilole unit is incorporated in polythiophene (polymers **62** and **63**), only weak performances are observed for single-layer devices (ITO/polymer/Mg-Ag).[57b] A series of 3,6-(dialkyl)silafluorene-based polymers **64**[57c](Figure 15) presenting a wide bandgap and ultraviolet light emission have been synthesized and were used as emitters in OLEDs. The monomer containing vinylene, anthracene, and tri-arylamine moieties incorporated into the poly(3,6-silafluorene) backbone can form efficient deep-blue emitting copolymers with EL efficiency of 1.1–1.9%. Furthermore electroluminescent poly(silole-co-germole)s containing borane/phosphine-ends **65** and **66** (Figure 15) have been synthesized in high yield and have similar emission properties (around 520 nm)[58]. The emission color of **65/66** mixture is green and the maximum brightness of the device is 2,760 cd/m2 with a luminous efficiency of 0.67 lm/W. In this case, the boranyl/phosphine end groups did not show an appreciable B-P-dative effect on the luminescent properties of poly(silole-co-germole) chain.

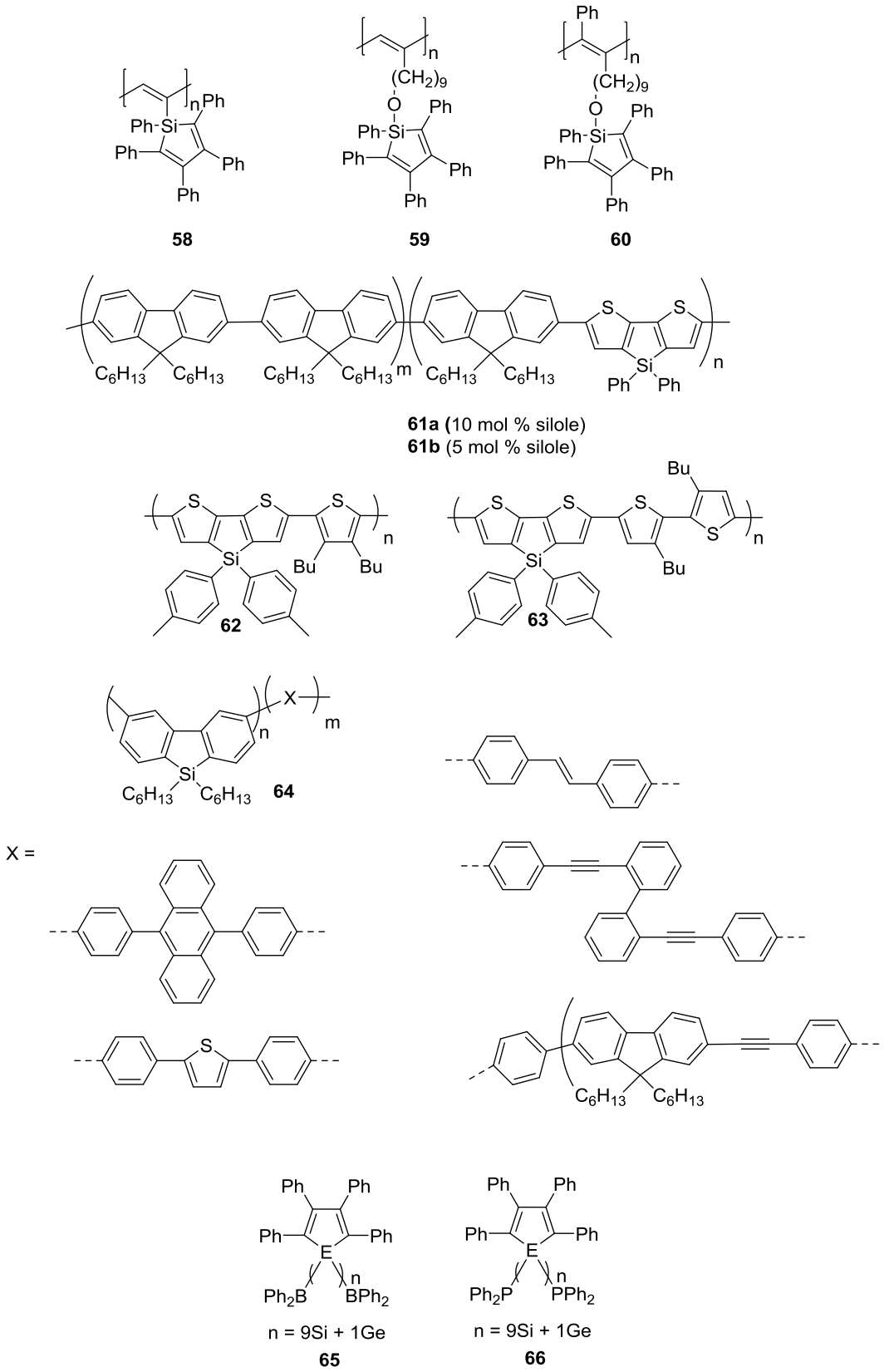

Figure 15. Chemical structures of polymers including siloles.

Photovoltaic cells (Organic solar cells (OSCs) and Dye-sensitized Solar Cells (DSSCs)

Fossil fuel alternatives, such as harvesting energy directly from sunlight using photovoltaic technology, are one of the ways to address growing global energy needs.[59] Since the discovery of silicon solar cells in the 1950's, tremendous advances in solar cell research and development have been made. DSSC and OSC devices are promising alternatives for producing clean and renewable energy, as there is the potential to fabricate them onto large areas of lightweight flexible substrates by solution processing at a low cost.
Actual organic/hybrid solar cells are mainly divided in two categories: DSSCs in which organic dyes are used for absorption light (the charge transport is insured by an inorganic semi-conductor such as TiO_2) followed by OSCs in which two organic materials (a donor and an acceptor) are used for both absorption of light and charge transport in a p-n junction.

Generally, a n-DSSC[60] device consists of four main components: a photoanode of transparent fluorine-doped tin oxide (FTO) glass covered with a wide bandgap nanocrystalline n-type semiconductor (TiO_2, ZnO, SnO_2, Nb_2O_5, etc.), a sensitizer (dye molecules, usually a push-pull organic dye or coordination complex) anchored on the surface of the semiconductor, a redox-coupled electrolyte (cobalt complexes, I^-/I_3^-…) and a counter electrode of FTO coated with platinum nanoparticles (Figure 16). Under irradiation, the chemisorbed dye is photo-excited to create exciton pairs, which are rapidly split at the nanocrystalline surface. The electrons are injected into the conduction band of the semiconductor and the holes, staying on the dyes, are recovered by the redox mediator in the liquid electrolyte. The oxidation state of the redox mediator is further recovered by electrons transferred from the counter electrode. A closed circuit is thereby established to continuously convert the solar light to electricity.

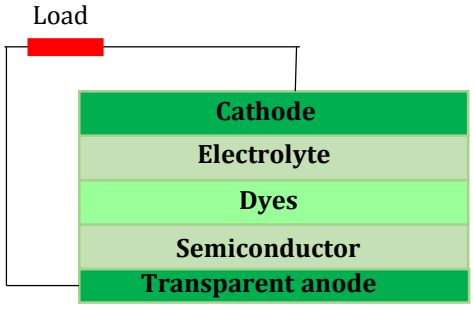

Figure 16: DSSC structure.

If the two semiconductors (n and p-type) are fully organic, the device is referred as an OSC. A bulk heterojunction (BHJ) OSC device consists of an active layer composed of a nanoscale blend of donor and acceptor materials sandwiched between two electrodes having different work

functions (Figure 17).[61,62] The general working principle first involves the photoexcitation of the donor material by the absorption of light to generate excitons. After the exciton dissociation/charge separation process at the donor–acceptor interface, the separated electrons and holes move towards their respective electrodes, driven by either the built-in electric field or the charge carrier concentration gradient, leading to a photocurrent or photovoltage.

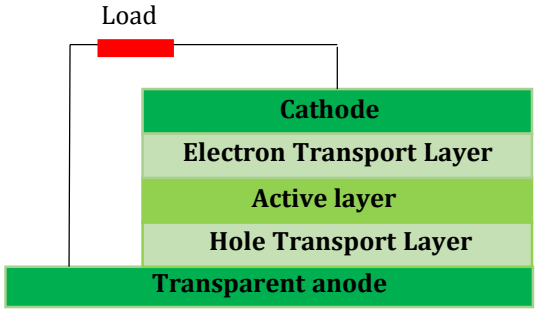

Figure 17. Structure of a bulk heterojunction OPV device.

For an organic material to be suited for SC applications, the compound must fulfill certain requirements. It must simultaneously possess strong absorption ability in the visible-near infrared spectral range, have suitable HOMO-LUMO energy levels to transfer electrons to the n-type semiconductor (or p-type in the case of an acceptor), have high hole or electron mobility and good film-forming properties in the case of OSC. Like in OLEDs, additional charge transport layers (such as ETL or cathode buffer layer) can be inserted in the devices.

To evaluate the performance of a PV device, some characteristic values are compared. They are all measured from the I/V curve as described in the Figure 18. Those values are the Power to Conversion efficiency (PCE) η (in %), the short-circuit current density J_{SC} (mA.cm^{-2}), the open circuit voltage V_{OC} (in V) and the fill-factor FF (without unity, maximal value = 1 or 100%).

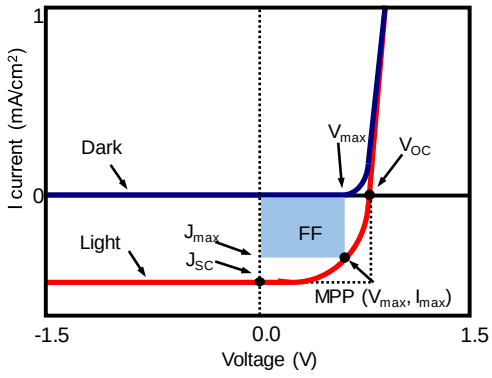

$$\eta = \frac{P_{out}}{P_{in}} = FF \frac{V_{OC} \times J_{sc}}{P_{in}}$$

$$FF = \frac{V_{max} \times J_{max}}{V_{OC} \times J_{sc}}$$

Figure 18. I/V curve of a PV device and characteristic values associated.

Dyes for dye-sensitized solar cells (DSSCs)

Matano/Imahori et al. used in 2010 a phosphole-based oligomer in a DSSC.[63] Their 1-hydroxy-1-oxodithienophosphole (**67**, Figure 19) was used as an accepting moiety, as well as a novel anchoring group. A PCE (η) of 1.8% was measured, together with a short-circuit current density (J_{sc}) of 7.4 mA cm^{-2}, an open-circuit voltage (V_{oc}) of 0.46 V, and a fill factor (FF) of 0.54. In 2014, the same authors developed a new push-pull based phosphole, featuring a triarylamine donor, terthiophene π-system, and a phosphole sulfide acceptor, bound to the semi-conductor through a carboxylic acid **68** (Figure 19).[64] The best PCE η was 5.6%, (J_{sc} of 12.5 mA cm^{-2}, a V_{oc} of 0.63V, and a FF of 0.70). Even if the efficiencies remain moderate, these examples highlight the versatility of using phospholes oligomers for future dyes in DSSCs.

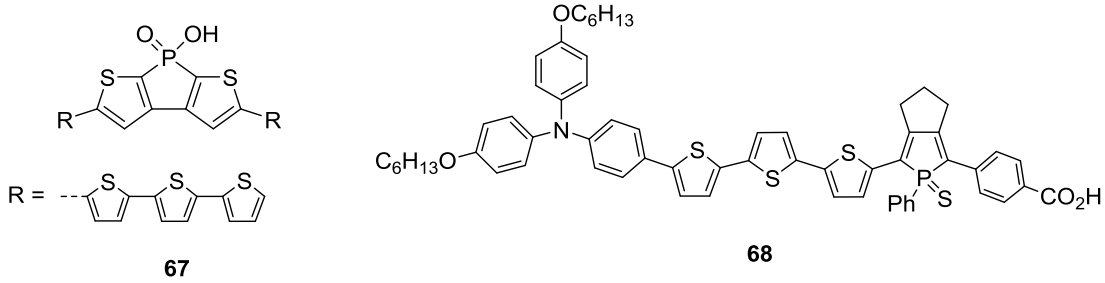

Figure 19. Phosphole-based dyes utilized in DSSCs.

Following the same strategy, silole-based oligomers were also prepared.[65] The best efficiency achieved with this strategy used compound **69** (Figure 20) featuring a triarylamine donor group, a π-backbone composed of EDOT-dithienosilole and a cyanoacrylic anchoring group.[66] A PCE of 10% could be obtained with a volatile electrolyte (J_{sc} : 17.94 mA cm^{-2}, V_{oc} : 0.73 V; FF: 0.73).

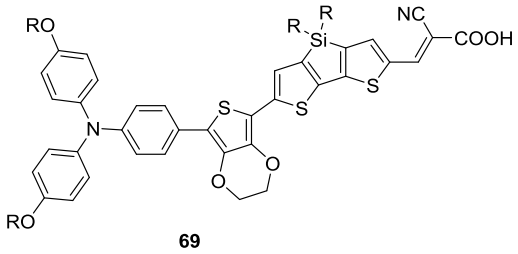

Figure 20. Silole-based dyes utilized in DSSCs.

Some P-containing materials were also tested as the electrolyte in DSSCs. To this end, phosphazenes were selected. Polyphosphazenes were first tested as electrolytes in Li-ion batteries.[67] Then, they were used as electrolytes in solid-states DSSCs. Electrolytes based on **70** (Figure 21) displayed good penetration into of TiO_2 and a PCE of 2.7% was obtained.[68] Pore penetration of phosphazenes was also studied by Allcock et al.[69] They showed that "small" polyphosphazenes such as **71** (Figure 21) help the penetration into the pores. However, low PCE were obtained.

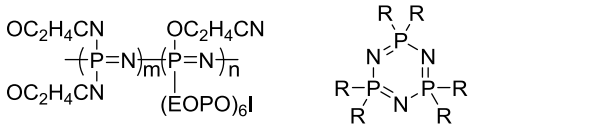

Figure 21. Structures of phosphazenes.

Donors in Organic Solar Cells (OSCs)

The first example of a phosphole-based copolymer used as a donor toward fullerene as acceptor in an OSC was published by Matano et al..[70] Polymers **72 - 73**, Figure 22, differ in the substituent on the P-atom either P=$NSO_2C_8H_{17}$ or P=O, Devices [ITO/PEDOT:PSS/**73**/$PC_{71}BM$/Al], showed low efficiency (PCE: 0.65%). However, the PCE of the device with **73** was an order of magnitude higher than with **72**, showing that the P-substituents play a key role. In 2015, it was demonstrated that the use of dithienophosphole oxide containing copolymers could generate highly efficient materials for OPV.[71] A BHJ incorporating polymer **74** (Figure 22) as the donor and $PC_{71}BM$ as the acceptor were prepared [ITO/PEDOT:PSS/polymer:$PC_{71}BM$ (1:4, weight ratio)/Ca/Al]. The best device performance had a PCE of 7.08% (V_{oc} = 0.85V, J_{sc} = 14.8 mA cm^{-2}, FF = 56.3%). It was highlighted that the polarizability of the dithienophosphole oxide moiety contributes to the high-excited state dipole moment, and thus facilitates the charge transfer to the acceptor. D-A copolymers with similar structure were also prepared (**75**, Figure 22) but with lower PCE in the devices.[72] As we will see in the next section, it must be kept in mind that the PCE in OSC depends on many factors (electronic/structural properties of the compounds, manufacturing processes of the cells, use of additives…) and it is difficult to make clear structure-properties relationships between the different polymers.

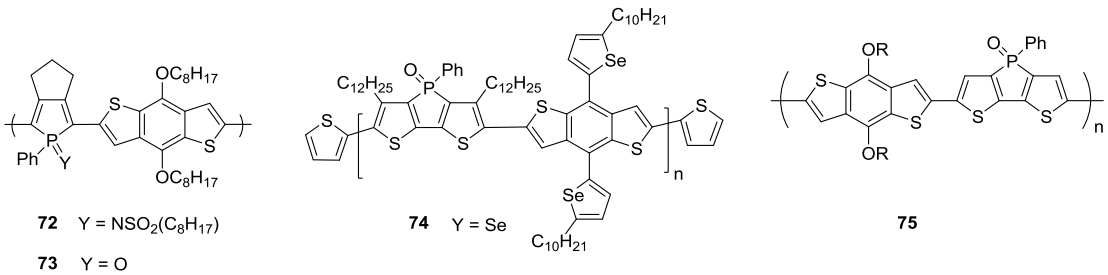

Figure 22. Phosphole containing polymers used for OSC devices.

Silole-based oligomers and polymers were also used as donors in BHJ solar cells together with fullerene derivatives. In particular, the use of donor-acceptor (D-

A) based copolymers, where dibenzosiloles/dithienosiloles are used as the D and various acceptors were used as the A, were found to be efficient. Hence, this D-A structure allows for efficient absorption of the UV-visible-NIR radiations, insuring good light harvesting properties.[73] Cao et al. prepared low-bandgap polymer **76** (Figure 23) based on a dibenzosilole-thiadiazole structure. The BHJ with PCBM as the acceptor led to a PCE of 5.4% (V_{oc} = 0.90 V, J_{sc} = 9.5 mA cm^{-2}, FF = 51%).[74] The mobility of the polymer (10^{-3} cm^2.V^{-1}.s^{-1}) appeared to be three times higher than its analogue when the SiR_2 part is replaced by CR_2. The replacement of the biphenyl unit of the dibenzosilole by a bithiophene gives a red-shift of the absorption. The D-A copolymer **77**, where the acceptor is a benzothiadiazole was prepared by Yang et al. (Figure 23).[75] This low-bandgap polymer possess good hole mobility (3.10^{-3} cm^2.V^{-1}.s^{-1}). Together with $PC_{71}BM$ used as n-semiconductor, a PCE of 5.1% was obtained in the BHJ (V_{oc} = 0.68V, J_{sc} = 12.7 mA cm^{-2}, FF = 55%). Photocurrent is generated over the whole visible range showing that both donor and acceptor absorption allows to fully cover the visible range. The modification of the acceptor in polymer **78** (Figure 23), where the thiadiazole is replaced by a thienopyrroledione, slightly increased the bandgap and the BHJ with $PC_{71}BM$ reached 7-8% PCE. [76,77] Several polymers based on this backbone were independently prepared and the PCE appeared to be sensitive to both aliphatic chains on the silicon atom, as well as the experimental conditions (solvent of evaporation, concentration, annealing temperature, additives…). However, this is not specific to siloles as BHJ efficiencies are known to depend on many interdependent factors linked with the preparation of the cells. When naphtha[2,3-c]thiophene-4,9-dione or polybithiopheneimide were used as the acceptor (polymers **79-80**, Figure 23), the efficiencies were still very high (PCE: 5.2% / 6.4%, respectively).[78,79]

The structural modifications are not limited to the accepting part. The donor can also be modified as in the silicon-bridged dithienocarbazole-based polymers (**81**, Figure 23).[80] Here again, good electron mobilities (up to 0.1 cm^2.V^{-1}.s^{-1}) and high PCE in BHJ devices with $PC_{71}BM$ as the acceptor (η = 5.2%; V_{oc} = 0.82 V, J_{sc} = 11.1 mA cm^{-2}, FF = 57 %) were measured.

These examples (this selection does not intend to be exhaustive) clearly show that preparing low bandgap polymers with dithienosiloles in the backbone is an efficient strategy for OPV materials.

Beside polymers, silole-containing oligomers were also prepared for OPV applications. In particular, the groups of G. Bazan/A. Heeger have been particularly active and successful in this area. In 2011, they reported a solution processable dithienosilole based oligomer (**82**, Figure 23). In a BHJ device with $PC_{71}BM$, a PCE of 6.7% was obtained using a very low amount of additives (V_{oc} = 0.78 V, J_{sc} = 14.4 mA cm^{-2}, FF = 59 %). Following this study, they reported several other examples of dithienosilole oligomers with efficiencies in the same order of magnitude.[81,82]

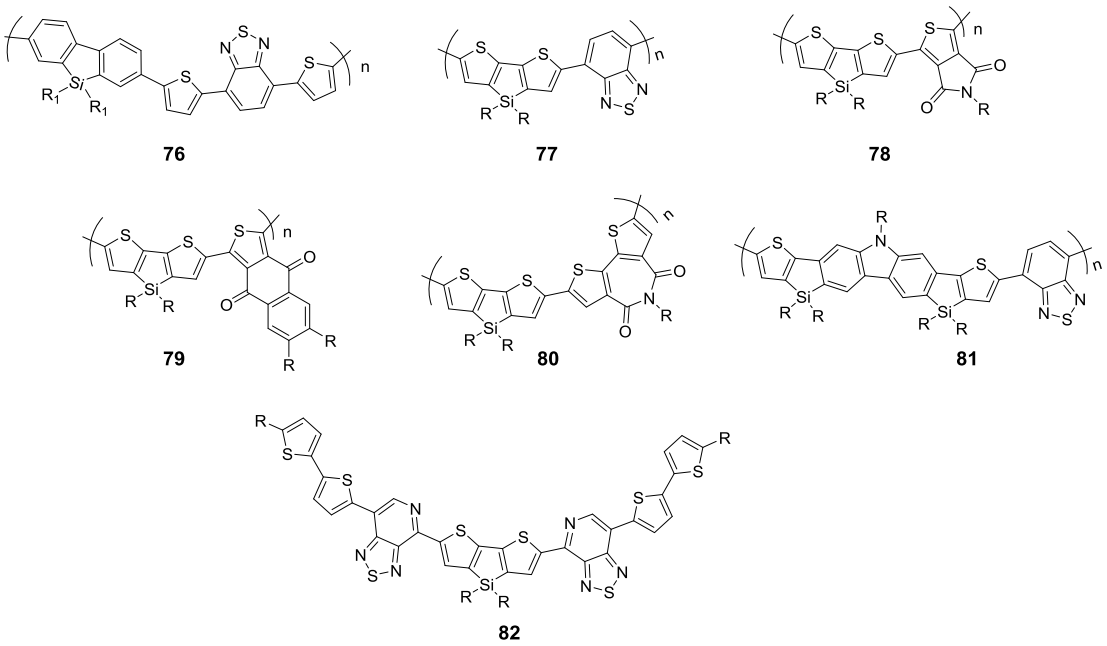

Figure 23. Si-based polymers used in OSCs.

Similarly to siloles, the first examples of Ge-based conjugated polymers used in optoelectronic devices were based on the dibenzogermole scaffold (**83**, Figure 24).[83] The compounds displayed decent hole mobility measured in OFET devices (0.04 $cm^2.V^{-1}.s^{-1}$) and good on/off ratio (10^6). Their efficiency in OSC with $PC_{71}BM$ was found to be 1.5% (V_{oc} = 0.76 V, J_{sc} = 4.1 mA cm^{-2}, FF = 62 %). Here also, the use of dithienogermole structures allowed to increase the efficiency of the devices. Homopolymers based on the dithienogermole monomer were first prepared.[84] They showed broad UV-vis absorption 500 nm<λ_{max}< 600 nm) and HOMO-LUMO level compatibles with applications in opto-electronics. Hole mobility in an OFET device was evaluated to be moderate (μ_{max} = 2.10-3 $cm^2.V^{-1}.s^{-1}$). The corresponding BHJ with $PC_{71}BM$ were also moderate (PCE = 1.7%). The rather low charge transport can be a reason for this efficiency. The first example of D-A copolymer based on dithienogermole was prepared by So/Reynolds et al. in 2012.[85] The alternating copolymer **84** absorbs until 735 nm which is similar to its Si-analog, but possesses a slightly higher HOMO. In an inverted BHJ with $PC_{71}BM$ as the acceptor, **84** displayed a PCE of 7.3% (V_{oc} = 0.85 V, J_{sc} = 12.6 mA cm^{-2}, FF = 68 %) while its Si-analog possessed a PCE of 6.6% under the same conditions. A PCE up to 8.5% could be obtained with the same polymer in slightly different conditions (V_{oc} = 0.86 V, J_{sc} = 15.9 mA cm^{-2}, FF = 63 %).[86] The fact that Ge-polymers display better performances than their Si-counterparts is sometime observed but is not a general trend. As in many studies about OPV, so many interdependent parameters are involved that it is complicated to draw direct conclusions between PCE and molecular structure. However, it is clear that both Si and Ge polymers allow to obtain high efficiencies in OPV devices. Most of the acceptors (thiadiazole, thienopyrroledione…) tested in the D-A structures for the dithienosiloles were also tested for the Ge-containing polymers and high efficiencies were also reported. [78,87]

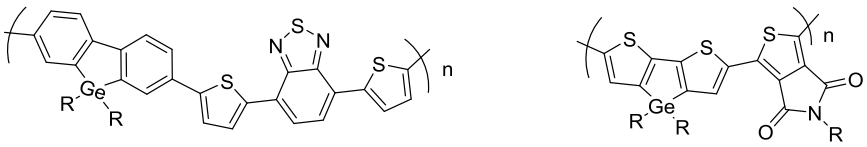

83 **84**

Figure 24. Ge-based polymers used in OSCs.

Silole-based polymers allow to obtain efficient OPV materials. This is partly due to the good ability of these materials to transport holes evaluated in organic field effect transistors (OFETs). In 2006, Fachetti/Marks and their co-workers developed dibenzosiloles/dithienosiloles based polymers **85** (Figure 25).[88] OFETs devices with a Si/SiO_2 wafer were prepared and showed good hole mobilities (0.05-0.08 $cm^2.V^{-1}.s^{-1}$) as well as on/off ratio of around $10^4/10^5$. Like for the OPV part, many variation of the polymer backbone were performed (for example polymer **86**, Figure 25).[89] In this study, various polymers with different monomeric units were prepared and compound **86**, with its complex monomer based on two dithienosilole units showed a moderate hole mobility (0.02 $cm^2.V^{-1}.s^{-1}$) with moderate on/off ratio (10^3). Mobility up to 0.1 $cm^2.V^{-1}.s^{-1}$ could be obtained with polymer **87**.[90] Many examples previously showed in the OPV section (Figure 25) were also studied in transistors, mainly to understand the charge transport in the solar cells.

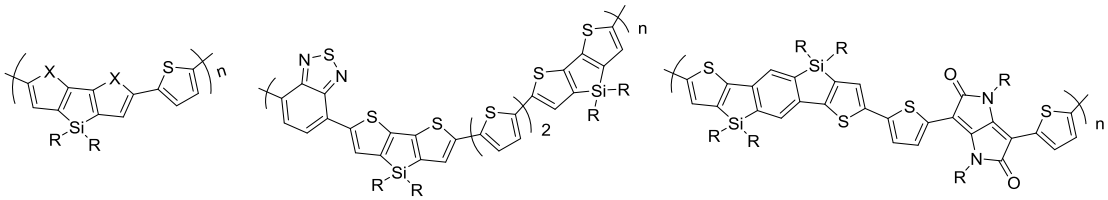

85a: X = CH=CH
85b: X = S

86 **87**

Figure 25. Si-based polymers used in OFETs.

This section demonstrates that phosphole/silole/germole-based conjugated oligomers/polymers possess strong UV-vis absorption together with good hole-transporting properties. They are thus highly interesting for applications in OPV and OFET devices. The fact that their efficiencies reached, particularly in OPV devices (~8%), corroborate this assumption. These novel conjugated polymers thus possess a bright future in this field.

Application in Electrochromic cells

Electrochromism is a phenomenon exhibited by some materials whose optical properties change when a potential is applied. In 2011, Baumgartner/Rodríguez-López et al. synthesized a dendritic material around a dithienophosphole **88** (Figure 26).[91] They constructed a device with the following configuration: [FTO/**88**/electrolyte (Bu_4NClO_4/THF 0.1M)/FTO].

When they applied a potential greater than 1.6V, the photoluminescence, under UV-light, of the film changed from orange to a light-green emission. This was the first time electrochromism was studied with a phosphorus heterocycle.

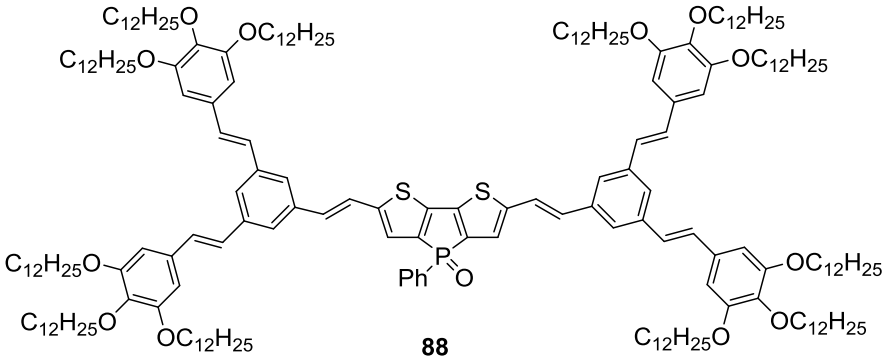

Figure 26. Phosphole containing material used for electrochromic devices.

Conclusion

This chapter surveys the main classes of heteroatom-containing polymers used in electronic devices. Only few polymers have made the cut to date and have been incorporated into electronic devices including organic light-emitting diodes (OLEDs), organic photovoltaic cells (OPV cells), dye-sensitized solar cells (DSSCs) and electrochromic cells. The chemistry of these π-conjugated systems with embedded heteroatom-moieties has been widely developed leading to a plethora of different structures. Structure-property relationships have still to be established in order to fully exploit the potential of heteroatom-moieties for the construction of conjugated frameworks. Nevertheless, it has already been clearly established that heavier atom derivatives offer specific advantages in comparison with their widely used carbon, sulfur or nitrogen analogues. There are many other heteroatom-scaffolds described in the literature (containing Bi, S, Te, or As..)[92, 93, 94, 95] which could potentially be used for the development of new efficient □-conjugated materials for optoelectronic applications. The next challenge is clearly to exploit these novel organic materials for the fabrication of optoelectronic devices.

Acknowledgements

This research is supported by the Ministère de la Recherche et de l'Enseignement Supérieure, Région Bretagne, the University of Rennes 1, CNRS, China-French associated international laboratory in "Functional Organophosphorus Materials". The COST Action CM1302 (SIPS) European Network on Smart Inorganic Polymers is also acknowledged.

Abbreviations

1D	one-dimensional
2D	two-dimensional
α-NPB	N,N′-Di(1-naphthyl)-N,N′-diphenyl-(1,1′-biphenyl)-4,4′-diamine
α-NPD	N,N′-Di(1-naphthyl)-N,N′-diphenyl-(1,1′-biphenyl)-4,4′-diamine
η	power conversion efficiency
A	ampere
Alq_3	tris-(8-hydroxyquinoline)aluminum
BCP	bathocuproine
BP	benzoporphyrin
BPhen	bathophenanthroline
BTPD-PFCB	bis- tetraphenylenebiphenyldiamine-perfluorocyclobutane
CBP	4,4'-N,N'-dicarbazolebiphenyl
CCT	correlated colour temperature
cd	candela
CIE	commission internationale de l'éclairage
cm	centimeter
CRI	Colour Rendering Index
CuPc	Copper(II) phthalocyanine
CPB	4,4'-N,N'-dicarbazole-biphenyl
DPVBi	4,4'-bis(2,2'-diphenylvinyl)biphenyl
DSSC	dye-sensitized solar cell
E_{red}	electrode potential (reduction)
E_T	triplet energy level
EL	electroluminescence
EML	emitting layer
ETL	electron transporting layer
ETM	electron transport material
eV	electron volt
$[(fbi)_2Ir(acac)]$	bis[2-(9,9-diethyl-9H-fluoren-2- yl)-1-phenyl-1H-benzimidazolate-κN,κC](acetylacetonato)- iridium(III)
FCNIrpic	bis[2-(5-cyano-4,6-difluorophenyl)pyridinato-C2,N](picolinato)iridium(III)
FET	field-effect transistor
FF	fill-factor
FIrpic	bis[2-(4,6-difluorophenyl)pyridinato-C^2,N](picolinato)iridium(III)
FCNIrpic	Bis[2-(5-cyano-4,6-difluorophenyl)pyridinato C2,N](picolinato) iridium(III)
FTO	fluorine-doped tin oxide
HOMO	highest occupied molecular orbital
Hfa	hexafluoroacetylacetonate
HTL	hole transporting layer

Ir(dbfmi)	mer-tris(N-dibenzofuranyl-N′-methylimidazole)iridium(III)
$Ir(mppy)_3$	(tris[2-(4-methyl-phenyl)- pyridine]iridium (III))
$Ir(ppy)_3$	tris[2-phenylpyridinato-C^2,N]iridium(III)
I	current
ITO	indium tin oxide
J_{sc}	short-circuit current
L	Luminance
lm	lumens
LUMO	lowest unoccupied molecular orbital
m	meter
MB	maximum brightness
mCP	N,N′-dicarbazolyl-3,5-benzene
Me	methyl
Mes	2,4,6-Trimethylphenyl- (=Mesityl-)
M_n	number-average molecular weight
η_L	luminous efficiency
η_{int}	internal quantum efficiency
η_{ext}	external quantum efficiency
η_P	luminous power efficiency or efficacy
NPB	N,N'-bis (naphthalen-1-yl)-N,N'-bis(phenyl)benzidine
ntfa	3-(2-naphthoyl)-1,1,1-trifluoroacetonate
OFET	organic field-effect transistor
OLED	organic light-emitting diode
OPV	organic photovoltaic cell
OSC	organic solar cell
P3HT	poly(3-hexylthiophene-2,5-diyl)
PBD	2-(4-biphenylyl)-5-(4-tert-butyl- phenyl)-1,3,4-oxadiazole
PCBM	[6,6]-phenyl C_{61} butyric acid methyl ester
$PC_{71}BM$	[6,6]-phenyl C_{71} butyric acid methyl ester
PCE	power conversion efficiency
PEDOT:PSS	poly(3,4-ethylenedioxythiophene)-poly(styrenesulfonate)
PhOLED	phosphorescent organic light-emitting diode
PLED	polymeric light-emitting diode
poly-TPD	poly(4-butylphenyl-diphenyl-amine)
PVK	poly N-vinylcarbazole
S	surface
s	second
SIMEF	bis(triorganosilymethyl)[60]fullerene
TADF	thermally activated delayed fluorescence
TTA	2-thenoyltrifluoroacetonate
V	volt
V_{oc}	open circuit voltage
W	watt
WOLED	white organic light-emitting diode

References

[1] a) K. Müllen, G. Wegner, *Electronic Materials: The Oligomer Approach*, Wiley-VCH, Weinheim, **1998**; b) T. A. Skotheim, J. R. Reynolds, *Handbook of conducting polymers*, 3rd ed., CRC, Boca Raton, Fla., **2007**; c) K. Müllen, U. Scherf, *Organic Light Emitting Devices: Synthesis, Properties and Applications*, Wiley-VCH, Weinheim, **2006**; d) S. Scholz, D. Kondakov, B. Lussem, K. Leo, *Chem. Rev.* **2015**, *115*, 8449; e) A. C. Grimsdale, K. L. Chan, R. E. Martin, P. G. Jokisz, A. B. Holmes, *Chem. Rev.* **2009**, *109*, 897; f) M. Gratzel, *Inorg. Chem.* **2005**, *44*, 6841; g) A. Hagfeldt, G. Boschloo, L. Sun, L. Kloo, H. Pettersson, *Chem. Rev.* **2010**, *110*, 6595; h) Y. J. Cheng, S. H. Yang, C. S. Hsu, *Chem. Rev.* **2009**, *109*, 5868; i) H. Sirringhaus, *Adv. Mater.* **2014**, *26*, 1319.

[2] a) A. Kraft, A. Grimsdale, A. B. Holmes *Angew. Chem. Int. Ed. Engl.* **1998**, *37*, 403; b) R. E. Martin, F. Diederich *Angew. Chem. Int. Ed. Engl.* **1999**, *38*, 1350; c) J. H. Burroughes, D. D. C. Bradley, A. R. Brown, R. N. Marks, K. Mackay, R. H. Friend, P. L. Burns, A. B. Holmes *Nature* **1990**, *347*, 539; d) F. Garnier, R. Haijaloui, A. Yassar, P. Srivastava *Science* **1994**, *265*, 1684.

[3] a) R. D. McCullough *Adv*. *Mater* **1998**, *10*, 93, b) U. Mitschke, P. Bäuerle *J. Mater. Chem.* **2000**, *10*, 1471, c) A. Toth, T. A. Schaub, U. Meinhardt, D. Thiel, J. Storch, V. Cirkva, P. Jakubic, D. M. Guldi, M. Kivala *Chem. Sci.* **2017**, *8*, 3494; d) O. Larranaga, C. Romero-Nieto, A. de Cozar *Chem. Eur. J.* **2017**, *23*, 17487

[4] (a) S. Yamagushi, Y. Itami, K. Tamao, *Organometallics* **1998**, *17*, 4910; (b) S. Yamagushi, T. Endo, M. Uchida, T. Izumizawa, K. Furukawa, K. Tamao, *Chem. Eur. J.* **2000**, *6*, 1683; (l) K. Tamao, S. Yamagushi, M. Shiozaki, Y. Nakagawa, Y. Ito, *J. Am. Chem. Soc.* **1992**, *114*, 5867.

[5] I. Albert, T. Marks, M. Ratner, *J. Am. Chem. Soc.* **1997**, *119*, 6575.

[6]. (a) N. Matsumi, K. Naka, Y. Chujo *J. Am. Chem. Soc.* **1998**, *120*, 10776; (b) N. Matsumi, K. Naka, Y. Chujo *J. Am. Chem. Soc.* **1998**, *120*, 5112.

[7] M. Hissler, P. W. Dyer, P. W., R. Réau, *Coord. Chem. Rev.* **2003**, *244*, 1.

[8] Some additionnal layers (hole blocking layer, electron blocking layers) can also be inserted to increase the performances.

[9] a) G. Farinola, R. Ragni, *Chem. Soc. Rev*., **2011**, *40*, 3467; b) S. R. Forrest, D. D. C. Bradley and M. E. Thompson, *Adv. Mater*., **2003**, *15*, 1043.

[10] A. B. Padmaperuma, G. Schmett, D. Fogarty, N. Washton, S. Nanayakkara, L. Sapochak, K. Ashworth, L. Madrigal, B. Reeves, C. W. Spangler, *MRS Proceedings* **2000**, *621*, Q3.9.1.

[11] M. Y. Ha, D. G. Moon, *Synth. Met.* **2008**, *158*, 617

[12] T. Oyamada, H. Sasabe, C. Adachi, S. Murase, T. Tominaga, C. Maeda, *Appl. Phys. Lett.* **2005**, *86*, 033503.

[13] I. Avilov, P. Marsal, J. L. Brédas, D. Beljonne, *Adv. Mater.* **2004**, *16*, 1624.

[14] a) S. O. Jeon, K. S. Yook, C. W. Joo, J. Y. Lee, *J. Mater. Chem.* **2009**, *19*, 5940; b) S. O. Jeon, K. S. Yook, C. W. Joo, J. Y. Lee, *J. Phys. D: Appl. Phys.* **2009**, *42*, 225103; c) S. O. Jeon, K. S. Yook, J. Y. Lee, S. M. Park, J. Won Kim, J.-H. Kim, J.-A. Hong, Y. Park, *Appl. Phys. Lett.* **2011**, *98*, 073306.

[15] S. O. Jeon, K. S. Yook, B. D. Chin, Y. S. Park, J. Y. Lee, *Sol. Energy Mat. Sol. Cells* **2010**, *94*, 1389.

[16] a) Y. Hasegawa, S. Natori, J. Fukudome, T. Nagase, T. Kobayashi, T. Nakanishi, Y. Kitagawa, K. Fushimi, H. Naito, *J. Phys. Chem. C* **2018**, 122, 9599 ; b) H. Xu, R. Zhu, P. Zhao, W. Huang, *J. Phys. Chem. C* **2011**, *115*, 15627.

[17] H. Tsuji, K. Sato, Y. Sato, E. Nakamura, *J. Mater. Chem.* **2009**, *19*, 3364.

[18] Y. Matano, A. Saito, Y. Suzuki, T. Miyajima, S. Akiyama, S. Otsubo, E. Nakamoto, S. Aramaki, H. Imahori, *Chem. Asian J.* **2012**, *7*, 2305.

[19] a) K. Tamao, M. Uchida, T. Izumizawa, K. Furukawa, S. Yamagushi, *J. Am. Chem. Soc*. **1996**, *118*, 11974; b) G. Yu, S. Yin, Y. Liu, J. Chen, X. Xu, X. Sun, D. Ma, X. Zhan, Q. Peng, Z. Shuai, B. Tang, D. Zhu, W. Fang, Y. Lu *J. Am. Chem. Soc*. **2005**, *127*, 6335; c) X. Zhan; C. Risko; F. Amy; C. Chan; W. Zhao; S. Barlow; A. Kahn; J.-L. Brédas; S. R. Marder; *J. Am. Chem. Soc.* **2005,** 127, 9021; d) s. h. Lee, B. B. Jang, Z. H. Kafafi, *J. Am. Chem. Soc.* **2005,** 127, 9071; e) H. Murata, G. G. Malliaras, M. Uchida, Y. Shen, Z. H. Kafafi, *Chem. Phys. Lett.* **2001**, *339*, 161.

[20] M. Uchida, T. Izumizawa, T. Nakano, S. Yamagushi, K. Tamao, , K. Furukawa *Chem Mater.,* **2001**, *13*, 2680.

[21] a) T. Noda, Y. Shirota *J. Am. Chem. Soc.* **1998,** 120, 9714; b) D. Tanaka, T. Tadeka, T. Chiba, S. Watanabe, J. Kido *Chem. Lett.* **2007**, *36*, 262

[22] P. E. Burrows, A. B. Padmaperuma, L. S. Sapochak, P. Djurovich, M. E. Thompson, *Appl. Phys. Lett.* **2006**, *88*, 183503.

[23] H. S. Son, C. W. Seo, J. Y. Lee, *J. Mater. Chem.* **2011**, *21*, 5638.

[24] S. Shao, J. Ding, T. Ye, Z. Xie, L. Wang, X. Jing, F. Wang, *Adv. Mater.* **2011**, *23*, 3570.

[25] H.-J. Jiang, Q.-W. Zhang, X. He, X.-L. Zhang, X. –W Zhang, Chinese Journal of Polymer Science **2017**, *35*, 611.

[26] S. Rothemund, I. Teasdale, *Chem. Soc. Rev.* **2016**, *45*, 5200.

[27] P. Schrögel, M. Hoping, W. Kowalsky, A. Hunze, G. Wagenblast, C. Lennartz, P. Strohriegl, *Chem. Mater.* **2011**, *23*, 4947

[28] M. S. Soh, S. A. G. Santamaria, E. L. Williams, M. Pérez-Morales, H. J. Bolink, A. Sellinger, *J. Polym. Sci. B Polym. Phys.* **2011**, *49*, 531.

[29] a) M. Matsumi, M. Miyata, Y. Chujo *J. Am Chem. Soc.* **1998**, *120*, 5112; b) M. Matsumi, M. Miyata, Y. Chujo *Macromolecules,* **1999**, *32*, 4467; c) M. Matsumi, M. Miyata, Y. Chujo *Macromolecules,* **2000**, *33*, 3956; d) M. Matsumi, M. Miyata, Y. Chujo *J. Am Chem. Soc.* **1998**, *120*, 10776; e) Y. Makioka, T. Hayashi, M. Tanaka *Chem. Lett*. **2004**, 33, 44; f) S.S.H. Mao, T.D. Tilley *Macromolecules,* **1997,** *30*, 5566; g) T. Baumgartner, T. Neumann, B. Wirges, *Angew. Chem. Int. ed.* **2004**, *43*, 6197; h) T. Baumgartner, W. Wilk *Org. Lett.* **2006**, *8*, 503; i) C. Xu, H. Yamada, A. Wakamiya, D. Yamaguchi, K. Tamao *Macromolecules,* **2004,** *37*, 8978; j) S. Yamaguchi, K. Tamao *Chem. Lett*, **2005**, 34, 2 ; k) C. Romero-Nieto, S. Durben, I. M. Kormos, *Adv. Funct. Mater.* **2009**, *19*, 3625

[30] C.-H. Chien, C.-K. Chen, F.-M. Hsu, C.-F. Shu, P.-T. Chou, C.-H. Lai, *Adv. Funct. Mater.* **2009**, *19*, 560

[31] C. Liu, Y. Gu, Q. Fu, N. Sun, C. Zhong, D. Ma, J. Qin, C. Yang, *Chem. Eur. J.* **2012**, *18*, 13828

[32] C. Liu, Y. Li, Y. Li, C. Yang, H. Wu, J. Qin, Y. Cao, *Chem. Mater.* **2013**, *25*, 3320

[33] S. Shao, J. Ding, L. Wang, X. Jing, F. Wang, *J. Am. Chem. Soc.* **2012**, *134*, 15189

[34] S. Shao, J. Ding, L. Wang, X. Jing, F. Wang, *J. Am. Chem. Soc.* **2012**, *134*, 20290.

[35] C. Fave, T. Y. Cho, M. Hissler, C. W. Chen, T. Y. Luh, C. C. Wu, R. Réau, *J. Am. Chem. Soc.* **2003**, *125*, 9254.

[36] H. C. Su, O. Fadhel, C. J. Yang, T. Y. Cho, C. Fave, M. Hissler, C. C. Wu, R. Réau, *J. Am. Chem. Soc.* **2006**, *128*, 983.

[37] B. Geffroy, N. Lemaitre, J. Lavigne, C. Denis, P. Maisse, P. Raimond, *Nonlinear Optics and Quantum Optics* **2007**, *37*, 9.

[38] a) O. Fadhel, M. Gras, N. Lemaitre, V. Deborde, M. Hissler, B. Geffroy, R. Réau, *Adv. Mater.* **2009**, *21*, 1261 ; b) D. Joly, D. Tondelier, V. Deborde, W. Delaunay, A. Thomas, K. Bhanuprakash, B. Geffroy, M. Hissler, R. Réau, *Adv. Funct. Mater.* **2012**, *22*, 567.

[39] a) P.-A. Bouit, A. Escande, R. Szűcs, D. Szieberth, C. Lescop, L. Nyulászi, M. Hissler, R. Réau, *J. Am. Chem. Soc.* **2012**, *134*, 6524; b) F. Riobé, R. Szűcs, P. A. Bouit, D. Tondelier, B. Geffroy, F. Aparicio, J. Buendia, L. Sanchez, R. Réau, L. Nyulászi, M. Hissler, *Chem. Eur. J.* **2015**, *21*, 6547.

[40] R. F. Chen, R. Zhu, Q. L. Fan, W. Huang, *Org. Lett.* **2008**, *10*, 2913.

[41] a) H. J. Bolink, S. G. Santamaria, S. Sudhakar, C. Zhen, A. Sellinger, *Chem. Commun.* **2008**, 618; b) H. J. Bolink, E. Barea, R. D. Costa, E. Coronado, S. Sudhakar, C. Zhen, A. Sellinger, *Org. Electron.* **2008**, *9*, 155.

[42] L. Brauge, G. Vériot, G. Franc, R. Deloncle, A.-M. Caminade, J.-P. Majoral, *Tetrahedron* **2006**, *62*, 11891.

[43] S. T. Kim, D.-H. Hwang, X.C. Li, J. Gruner, R. H. Friend, A.B. Holmes, H.K. Shim Adv. Mater. **1996**, *8*, 979

[44] S. Hoeger, J. McNamara, S. Schricker, F. Wudl, Chem Mater. **1994**, *6*, 171

[45] C. Zhang, S. Hoeger, K. Pakbaz, F. Wudl, A. J. Heeger, *J. Electron. Mater.* **1994**, *23*, 453.

[46] Z. Chen, W. Huang, L. Wang, E. Kang, B.J. Chen, C.S.Lee, S.T. Lee *Macromolecules,* **2000**, *33*, 9015

[47] T. Ahn, S. Ko, J. Lee, H. Shim *Macromolecules,* **2002**, *35*, 3495

[48] S. Jin, M. Jang, H. Suh *Chem. Mater.* **2002**, *14*, 643

[49] Y. Jin, S. Song, S. H. Park, J.-A. Park, J. kim, H. Y. Woo, K. Lee, H. Suh *Polymer* **2008**, *49*, 4559

[50] D.-H. Hwang, J.-I. Lee, N.-S. Cho, H.-K. Shim *J. Mater. Chem.* **2004**, *14*, 1026

[51] a) R.O. Garay, B. Mayer, F.E. Karasz, R. W. Lenz *J. Polym. Sci. A.***1995**, *33*, 525; b) R.E. Martin, F. Geneste, B. S. Chuah, C. Fischmeister, Y. Ma, A. B. Holmes, R. Riehn, F. Cacialli, R. H. Friend *Synth. Met*. **2001**, *122*, 1; c) B. S. Chuah, F. Geneste, A. B. Holmes, R.E. Martin, H. Host, , F. Cacialli, R. H. Friend, H.-H. Horhold, S. Pfeiffer, D.-H. Hwang *Macromol. Symp.* **2000**, *154*, 177.

[52] a) H.-K. Kim, M.-K. Ryu, K.-D. Kim, S.-M. Lee, S.-W. Cho, J.-W. Park *Macromolecules* **1998**, *31*, 1114, b) K.-D. Kim, J.-S. Park, H.-K. Kim, T.B. Lee, K. T. No *Macromolecules* **1998**, *31*, 7267

[53] a) G.G. Malliaras, J. K. Herrema, J. Wildeman, R. H. Wieringa, R.E. Gill, S. S. Lampoura, G. Hadziioannou *Adv. Mater.* **1993**, *5*, 721; b), J. K. Herrema, P. F. van Hutten, R.E. Gill, J. Wildeman, R. H. Wieringa, G. Hadziioannou *Macromolecules* **1995**, *28*, 8102.

[54] K. Yoshino, M. Hirohata, T. Sonoda, R. Hidayat, A. Fujii, A. Naka, M. Ishikawa, *Synth. Met.* **1999**, *102*, 1158.

[55] a) B. Z. Tang, A. Qin, Eds.; Wiley, **2013**; b) Y. Hong, J. W. Y. Lam, B. Z. Tang, *Chem. Soc. Rev.* **2011**, *40*, 5361-5388; c) J. Mei, N. L. C. Leung, R. T. K. Kwok, J. W. Y. Lam, B. Z. Tang, *Chem. Rev.* **2015**, *115*, 11718−11940.

[56] J. Chen, Z. Xie, J. W. Y. Chen, C. C. W. Law, B. Z. Tang *Macromolecules* **2003**, *36*, 1108.

[57] a) M.S. Liu, J. Luo, A. K. Y. Len *Chem. Mater* **2003**, *15*, 3500; b) J. Ohshita, K. Kimura, K.-H. Lee, A. Kunai, Y. W. Kwak, E.-C. Son, Y. Kunugi *J. Polym. Sci. Part A; Polym. Chem.* **2007**, *45*, 4588; c) Y. Q. Mo, X. Y. Deng, X. Jiang, Q. H. Cui *J. Polym. Sci. Part A; Polym. Chem.* **2009**, *47*, 3286; d) L. Liao, A. Cirpan, Q. Chu, F. E. Karasz, Y. Pang *J. Polym. Sci. Part A; Polym. Chem.* **2007**, *45*, 2048.

[58] S.-H. Roh, H. Cheong, J. Park, H. Sohn, M.-S. Cho, H.-G. Woo *J. Nanosci. Nanotechnol.* **2014**, *14*, 6438

[59] (a) C. J. Brabec, N. S. Sariciftci and J. C. Hummelen, *Adv. Funct. Mater.*2001, **11**, 15 ; (b) S.Günes, H. Neugebauer and N. S. Sariciftci, *Chem. Rev.* 2007, **107**, 1324 ; (c) W. Cao and J. Xue, *Energy Environ. Sci.*, 2014, **7**, 2123 ; (d) H.-Y. Chen, D.-B. Kuang and C.-Y. Su, *J. Mater. Chem.,* 2012, **22**, 15472.

[60] (a) M. Grätzel, *Inorg. Chem* 2005, **44**, 6841. ; (b) A. Hagfeldt, G. Boschloo, L. Sun, L. Kloo and H. Petterson, *Chem. Rev.* 2010, **110**, 6595.

[61] Y.-Y. Cheng, S.-H. Yang, C. S. Hsu, *Chem Rev* 2009, **109**, 5968.

[62] J. L. Delgado, P.-A. Bouit, S. Fillipone, M.A. Herranz and N. Martín, *Chem. Commun.* 2010, **46**, 4853.

[63] A. Kira, Y. Shibano, S. Kang, H. Hayashi, T. Umeyama, Y. Matano, H. Imahori, *Chem. Lett.* **2010**, *39*, 448.

[64] Y. Matano, Y. Hayashi, H. Nakano, H. Imahori, *Heteroatom Chem.* **2014**, *25*, 533.

[65] L.-Y. Lin, C.-H. Tsai, K.-T. Wong, T.-W. Huang, L. Hsieh, S.-H. Liu, H.-W. Lin, C.-C. Wu, S.-H. Chou, S.-H. Chen, A.-I. Tsai, *J. Org. Chem.* **2010**, 75, 4778–4785.

[66] W. Zeng, Y. Cao, Y. Bai, Y. Wang, Y. Shi, M. Zhang, F. Wang, C. Pan, P. Wang, *Chem. Mater.* **2010**, 22, 1915–1925.

[67] P. M. Blonsky, D. F. Shriver, P. Austin, H. R. Allcock, *J. Am. Chem. Soc.* **1984**, *106*, 6854

[68] W. Xiang, Y. Zhou, X. Yin, X. Zhou, S. Fang, Y. Lin, *Electrochim. Acta* **2009**, *54*, 4186.

[69] S.-T. Fei, S.-H. A. Lee, S. M. Pursel, J. Basham, A. Hess, C. A. Grimes, M. W. Horn, T. E. Mallouk, H. R. Allcock, *J. Power Sources* **2011**, *196*, 5223.

[70] Y. Matano, H. Ohkubo, T. Miyata, Y. Watanabe, Y. Hayashi, T. Umeyama, H. Imahori, *Eur. J. Inorg. Chem.* **2014**, *2014*, 1620.

[71] K. H. Park, Y. J. Kim, G. B. Lee, T. K. An, C. E. Park, S.-K. Kwon, Y.-H. Kim, *Adv. Funct. Mater.* **2015**, *25*, 3991.

[72] T. T. T. Bui, S. Park, Q. V. Hoang, C. E. Song, S. K. Lee, J.-C. Lee, S.-J. Moon, W. S. Shin, *Synth. Met.* **2016**, *215*, 235.

[73] P. L. T. Boudreault, A. Michaud, M. Leclerc, *Macromol. Rapid Commun*. **2007**, 28, 2176.

[74] E. Wang, L. Wang, L. Lan, C. Luo, W. Zhuang, J. Peng, Y. Cao, *Appl. Phys. Lett.* **2008**, 92, 033307–033303.

[75] J. Hou, H.-Y. Chen, S. Zhang, G. Li, Y. Yang, *J. Am. Chem. Soc.* **2008**, 130, 16144..

[76] T.-Y. Chu, J. Lu, S. Beaupré, Y. Zhang, J.-R. Pouliot, S. Wakim, J. Zhou, M. Leclerc, Z. Li, J. Ding, Y. Tao, *J. Am. Chem. Soc.* **2011**, 133, 4250.

[77] T.-Y. Chu, J. Lu, S. Beaupré, Y. Zhang, J.-R. Pouliot, J. Zhou, A. Najari, M. Leclerc, Y. Tao, *Adv. Funct. Mater.* **2012**, 22, 2345.

[78] X. Guo, N. Zhou, S. J. Lou, J. W. Hennek, R. Ponce Ortiz, M. R. Butler, P.-L. T. Boudreault, J. Strzalka, P.-O. Morin, M. Leclerc, J. T. López Navarrete, M. A. Ratner, L. X. Chen, R. P. H. Chang, A. Facchetti, T. J. Marks, *J. Am. Chem. Soc.* **2012**, 134, 18427–18439

[79] C. Cui, X. Fan, M. Zhang, J. Zhang, J. Min, Y. Li, *Chem. Commun*. **2011**, 47, 11345

[80] J.-S. Wu, Y.-J. Cheng, T.-Y. Lin, C.-Y. Chang, P.-I. Shih, C.-S. Hsu, *Adv. Funct. Mater.* **2012**, 22, 1711

[81] T. S. van der Poll, J. A. Love, T. Q. Nguyen, G. C. Bazan, *Adv. Mater.* **2012**, 24, 3646

[82] A. K. K. Kyaw, D. H. Wang, V. Gupta, J. Zhang, S. Chand, G. C. Bazan, A. J. Heeger, *Adv. Mater.* **2013**, 25, 2397

[83] N. Allard, R. B. Aïch, D. Gendron, P.-L. T. Boudreault, C. Tessier, S. Alem, S.-C. Tse, Y. Tao, M. Leclerc, *Macromolecules*, **2010**, 43, 2328.

[84] J. Ohshita, M. Miyazaki, D. Tanaka, Y. Morihara, Y. Fujita, Y. Kunugi, *Polym. Chem.*, **2013**, 4, 3116

[85] C. M. Amb, S. Chen, K. R. Graham, J. Subbiah, C. E. Small, F. So, J. R. Reynolds, *J. Am. Chem. Soc.*, **2011**, 133, 10062.

[86] I. Constantinou, T.-H. Lai, D. Zhao, E. D. Klump, J. J. Deininger, C. K. Lo, J. R. Reynolds, F. So, *ACS Appl. Mater. Interfaces*, **2015**, 7, 4826

[87] Q. Wang, S. Zhang, L. Ye, Y. Cui, H. Fan, J. Hou, *Macromolecules*, **2014**, 47, 5558

[88] H. Usta, G. Lu, A. Facchetti, T. J. Marks, *J. Am. Chem. Soc.* **2006**, 128, 9034.

[89] P. M. Beaujuge, W. Pisula, H. N. Tsao, S. Ellinger, K. Müllen, J. R. Reynolds, *J. Am. Chem. Soc.* **2009**, 131, 7514

[90] R. S. Ashraf, Z. Chen, D. S. Leem, H. Bronstein, W. Zhang, B. Schroeder, Y. Geerts, J. Smith, S. Watkins, T. D. Anthopoulos, H. Sirringhaus, J. C. de Mello, M. Heeney, I. McCulloch, *Chem. Mater.* **2011**, 23, 768–770.

[91] C. Romero-Nieto, M. Marcos, S. Merino, J. Barbera, T. Baumgartner, J. Rodriguez-Lopez, *Adv. Funct. Mater.* **2011**, *21*, 4088.

[92] J. Linshoeft, E.J. Baum, A. Hussain, P.J. Gates, C. Naether and A. Staubitz, *Angew. Chem. Int. Ed.* **2014**, *53*, 12916

[93] G. He, L. Kang, W. Torres Delgado, O. Shynkaruk, M. J. Ferguson, R. McDonald, E. Rivard, *J. Am. Chem. Soc.*, **2013**, *135*, 5360

[94] S. M. Parke, Mary A. B. Narreto, E. Hupf, R. McDonald, M. J. Ferguson, F. A. Hegmann, E. Rivard, *Inorg. Chem.* ***2018*** 10.1021/acs.inorgchem.8b00149.

[95] J. P. Green, Y. Han, R. Kilmurray, M. A. McLachlan, T. D. Anthopoulos, M. Heeney, *Angew. Chem., Int. Ed.* **2016**, *55*, 7148–7151.